Transportation Research Part B 186 (2024) 102994

Contents lists available at ScienceDirect

Transportation Research Part B

journal homepage: www.elsevier.com/locate/trb

How mandatory are 'Mandatory' lane changes? An analytical and experimental study on the costs of missing freeway exits

Zhaohan Wang *, Mohsen Ramezani, David Levinson

The University of Sydney, School of Civil Engineering, Australia

ARTICLE INFO

Keywords:
Traffic flow theory
Freeway exit ramp
Travel cost
Network resilience

ABSTRACT

Lane changing, recognised as one of the most intricate manoeuvres in road traffic, has attracted extensive scholarly interest. To date, the concept of lane change has been categorised into two distinct classifications, namely mandatory and discretionary. Mandatory lane changes (MLCs) are often regarded as absolute, implying that the possibility of not executing the lane change is frequently disregarded. This paper questions this widely accepted proposition by evaluating the costs of neglecting an MLC. Specifically, we examine the costs associated with not making MLCs for exiting freeways, effectively quantifying the cost of missing such exits. The core of this study involves a dual approach comprising an analytical model for the costs of missing exits alongside an empirical analysis of two GPS datasets from the Minneapolis - St. Paul metropolitan area. The performance of the analytical model is validated by cross-referencing it against exit-missing costs from the top 50 metropolitan areas in the US. Regarding the empirical study, it was found that while both time and distance costs are associated with missing exits, the magnitudes of these costs are not substantial. The results obtained in this study offer novel insights into the nature of MLC, and we argue that future models should consist of discretionary (DLC), mandatory (MLC), and *expedient* (ELC) lane changes. Moreover, the analytical model developed in this study can be integrated into the trade-off function of an ELC model, enabling drivers to bypass their intended exit when needed.

1. Introduction

As one of the most common microscopic road manoeuvres, lane change has attracted considerable research interest, e.g. Ji and Levinson (2020) among others. Poorly executed lane changes can cause flow oscillations and traffic incidents that may incur social and economic costs. More severe impacts are often observed under heavier traffic conditions with the potential of flow breakdowns under extreme cases (Ahn and Cassidy, 2007; Zheng et al., 2013; Gao and Levinson, 2023). Therefore, the development of precise lane change models is a crucial step for understanding the fundamental characteristics of traffic flow.

Based on its motivation, the notion of lane change has traditionally been classified as discretionary or mandatory. Discretionary lane change (DLC) occurs when the driver perceives that the target lane offers superior driving conditions compared to the current one. This encourages the driver to change lanes in aspiration of speed and safety advantages. Mandatory lane change (MLC), on the other hand, applies when the driver must leave the current lane, in order to avoid obstructions downstream (e.g., lane drop) or moving to the appropriate lane in preparation for future turning movements.

The idea of categorising various lane change types was first introduced by Gipps (1986), who proposed a rule-based model that assesses the possibility, necessity, and desirability of a lane change before outputting a binary result of whether to change or not.

* Corresponding author.
E-mail address: zhaohan.wang@sydney.edu.au (Z. Wang).

https://doi.org/10.1016/j.trb.2024.102994
Received 16 April 2023; Received in revised form 19 May 2024; Accepted 30 May 2024

Although the model does not explicitly define MLC and DLC, the author designated a hierarchical structure of lane change decisions based on the motivation of changing lanes. Halati et al. (1997) extended upon Gipps' model and classified lane changes as DLC and MLC. MLCs are performed when the driver must leave the current lane, such as avoiding lane blockage or use downstream off-ramp. DLCs are performed when the driver perceives the target lane has better driving conditions but are not required to do so. Yang and Koutsopoulos (1996) likewise, developed a micro-simulator based on Gipps' model. In their model, MLCs are triggered to bypass downstream blockage, connect to path link, obey lane-use regulations, and respond to signs. DLCs are performed when the speed of the leader is below a desired speed. Ahmed (1999) developed a discrete choice framework to model three lane-changing steps: decision to consider a lane change, choice of a target lane, and gap acceptance. A forced merging model that captures forced lane changing behaviour and courtesy yielding is developed. DLCs are only considered when MLCs conditions do not apply.

To account for the sudden transition from DLC to MLC, Toledo et al. (2003) proposed an integrated approach where DLC and MLC are jointly considered in a single utility model. The relative importance between the two depends on a number of explanatory variables, including the surrounding vehicle states, future path plans, network knowledge, and driving styles. Later in Toledo et al. (2005), the authors saw the research gap that existing models do not explicitly incorporate the choice of a target lane, which may require a sequence of lane changes. Consequently, they propose an approach that evaluates the utility of each lane as the target, based on a number of attributes, such as the lane speed and density, presence of heavy vehicles, and future path planning variables. The execution of the lane change is determined using a gap acceptance model with spatial information between the subject vehicle and its lead and lag vehicles in the adjacent lane.

Extending on the integrated DLC and MLC model, Toledo et al. (2007) presents a framework that captures inter-dependencies between lane changing and acceleration and takes into account drivers' planning capabilities. The proposed driving behaviour model is based on the concepts of short-term goals and short-term plans. The short-term goal is defined as a target lane, which is the lane that the driver perceives as best to be in. Down a hierarchy is the short-term plan, which is defined by a target gap that the driver intends to use to change lane. Finally, to facilitate the short-term plan, the driver applies an acceleration. Schakel et al. (2012) proposed a lane change model centred around the idea of lane change desire. The desire follows from the trade-off between route, speed, and keep right incentives. As lane change desire increases, drivers become more assertive. Four levels of lane change desire are formulated, from lowest to highest, the lane changer performs: no lane change; lane change only in a free fashion; synchronisation with target lane to prepare for lane change; lane change indication to create gap. Relaxation is implemented as drivers accept smaller time headways for large desire. Other game-theoretic methods (Kita, 1999; Zhang et al., 2020), machine learning methods (Hunt and Lyons, 1994; Hou et al., 2014), and artificial intelligence simulation models like fuzzy logic models (Hou et al., 2012) were also developed to investigate human preferences of MLC. For a systematic review of lane change and gap acceptance, please refer to Zheng (2014).

In summary, numerous lane change models have been proposed in the literature. However, it is common for these models to tacitly accept that MLCs are absolute, meaning that the possibility of not performing the lane change is often overlooked. While this proposition holds true in scenarios where the driver must make a lane change decision (e.g., changing lanes to avoid a blockage), its validity is questionable in scenarios that are not as restrictive (e.g., changing lanes for tactical routing). In this paper, we study what would be the cost for not making a lane change, which consequently reflects the level of mandatoriness of a lane change maneuver. We specifically focus on the tactical routing scenario, examining lane changes made to diverge onto a freeway off-ramp. Hence, the study is conducted on the cost of not making the lane change decision at that exiting point and tries to corroborate "how costly would this misstep be". It should be noted, the lane change we focus on in this paper is centred around the combined concepts of lane change decision and execution. We assume that a lane change decision directly indicates whether a lane change has been executed and, consequently, whether the vehicle has taken the correct off-ramp. Thus, the problem transforms to examining the costs associated with missing off-ramps.

We start by formulating the exit-missing costs analytically by decomposing the costs into sub-components on the freeway and surface street network levels. Through utilising probability theory and stochastic geometry, the costs can be approximated with simple variables derived from the network structures. The proposed model is then validated using simulation data from the Longitudinal Employer-Household Dynamics (LEHD) Census dataset (US Census Bureau, 2022a) for the top 50 metropolitan areas in the US.

In addition, we conduct an empirical investigation using two large-scale GPS datasets from the Minneapolis - St. Paul metropolitan region. Real-life GPS data are considered vital for gaining insight into drivers' decision-making processes, and as such, it is critical in analysing actual exit-missing costs. The datasets in this study were collected at high sampling rates and include comprehensive GPS trajectories.

Both the analytical and empirical results indicate that the additional costs associated with not executing lane changes to exit freeways are generally on the order of minutes and kilometres. Compared with lane changes performed to avoid obstacles, lane changing for tactical routing has lower mandatoriness. This may partially explain why drivers are sometimes prone to missing their scheduled turns. From a modelling perspective, models should account for the likelihood of drivers missing exits, which could be due to factors such as tiredness, distractions, or miscalculations regarding the ease of lane change maneuvers. From a design perspective, this study could be particularly useful in informing lane change decisions at the route choice level.

Findings of this paper suggest that future research could investigate lane change models that distinguish between three categories: discretionary, expedient (ELC), and mandatory, where the benefits of changing lanes are on the order of seconds/metres, minutes/kilometres, and infinite, respectively. In this paper, we define ELC as lane changes performed only for tactical routing. All other previously defined MLCs remain in the MLC category. Lane changes made to avoid downstream obstacles are considered MLCs because the cost of not executing such a lane change would, intuitively, be infinite. If no lane change decisions are made, the drivers

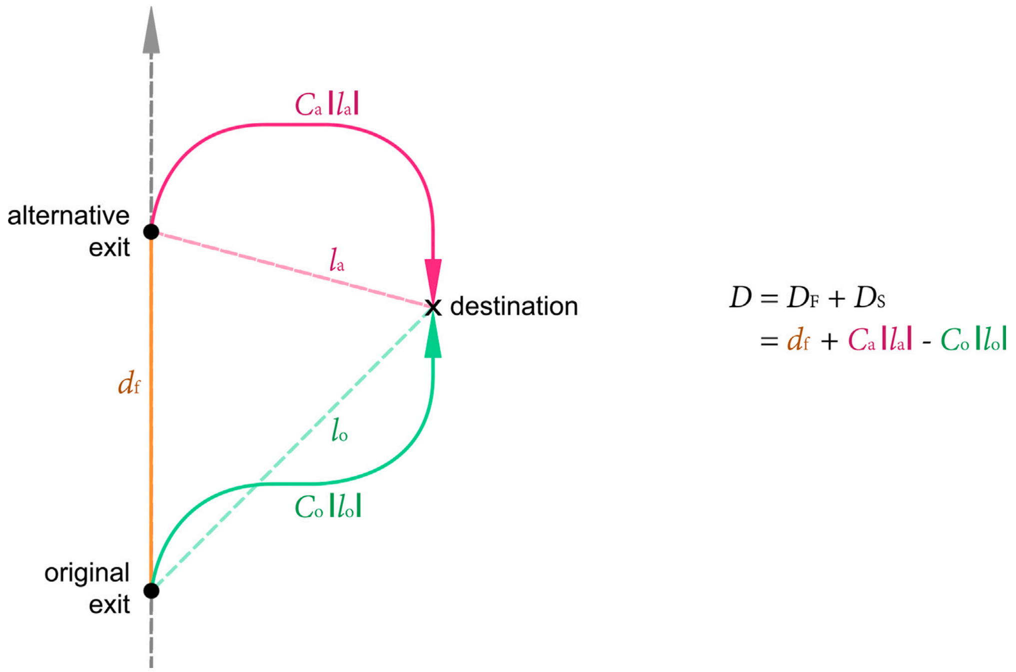

Fig. 1. Diagram illustrating the composition of the costs. In this case, the vehicle moves in an upward direction along the freeway, indicated by the grey dashed line. The pink and green routes denote the paths from the exits on the freeway to the destination (marked as a cross). The orange line corresponds to the section of the freeway located between the two exits. The cost incurred due to missing the original exit and subsequently taking the alternative exit is equal to the combined length of the orange line and the disparity between the lengths of the pink and green lines. (For interpretation of the references to colour in this figure legend, the reader is referred to the web version of this article.)

could be stuck indefinitely. Other previously defined MLCs, such as obeying lane usage indications or yielding to emergency vehicles, remain in the MLC category until further verification of their costs. However, we hypothesise that they might be better classified as ELCs since drivers sometimes choose not to make these lane changes. Drivers often weigh the trade-offs between changing lanes and not changing lanes before making decisions.

The rest of the article is organised as below. Section 2 introduces our analytical model for the exit-missing costs. The performance of the model is validated in Section 3 using simulated costs from the US. In Section 4, our empirical study is explicated, outlining the methodology, as well as presenting the result outcomes and corresponding discussions. Finally, in Section 5, this paper concludes by summarising the research findings, the limitations, and the implications for future studies.

2. Analytical costs for missing freeway exits

To adequately address the nature of the exit-missing cost, we break it down and solve it analytically. By applying probability theory and stochastic geometry, the actual figures can be estimated by feeding some network-level variables into the model. A summary table of notation conventions is provided in Appendix A.

2.1. Mean of exit-missing costs

Our study initially investigates the distance cost incurred due to missed exits. This cost, expressed as the extra travel distance (D), can be subdivided into two distinct components: the freeway level cost (D_F) and the surface street level cost (D_S). D_F is simply the gap length between the alternative and the original exits, whereas D_S represents the discrepancy between the distance travelled from the alternative exit to the destination and the distance travelled from the original exit to the destination. The corresponding travel distances on the surface street network can be further decomposed to the circuities (C_a and C_o) multiplying the Euclidean distances ($|l_a|$ and $|l_o|$) from the exits to the destination. Circuity is defined as the ratio between the route length and the Euclidean distance for an OD pair (Axhausen et al., 2003). Fig. 1 visualises these relationships.

Extending the aforementioned approach to encompass multiple trips over a region, the formulation transforms into determining the average distance cost by calculating the mean of its constituent parts. While the average gap length and the average circuity can be computed with relative ease, estimating the average Euclidean distance between a destination and its original or alternative exits presents a challenge, as the location of the destination is a random variable, and the distance is contingent upon it. To tackle this issue, we assume that people use a pool of nearby exits to reach their locations and subsequently determine the proportion of trips

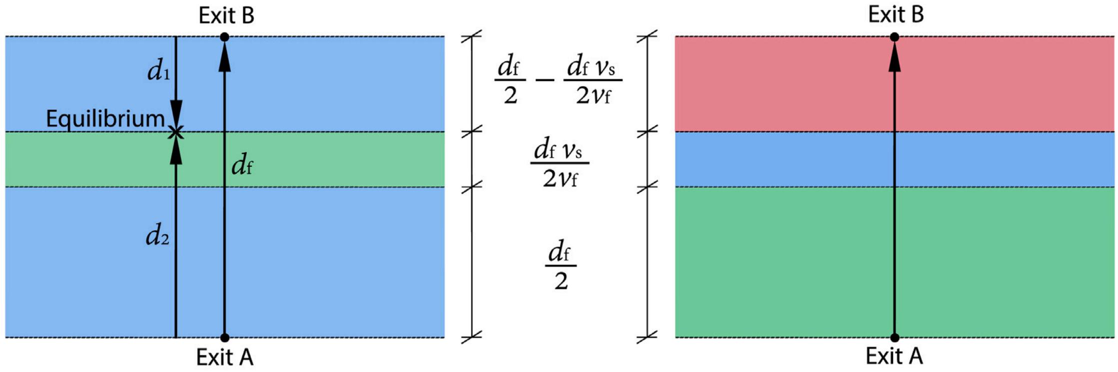

(a) Original scenario (b) Alternative scenario

Fig. 2. Diagram showing the contribution of exits to the surrounding destinations. The blue regions indicate that destinations within this area are reached from their nearest exit, the green area corresponds to the second nearest exit, and the red area corresponds to the third nearest exit. Subgraph (a) shows the contribution of exits for the original route while (b) shows the contribution of exits for the alternative route, which we assume that drivers have missed their intended exits. (For interpretation of the references to colour in this figure legend, the reader is referred to the web version of this article.)

that belong to each exit. Next, we calculate the average Euclidean distance of the exits, and this value, when considered alongside their proportion of usage, forms the measure of the average distance to the alternative and original exits.

Suppose that freeways can be subdivided into segments at exits. For one arbitrary segment (see Fig. 2), the percentage of people travelling to the nearest (1st order) and 2nd nearest (2nd order) exits can be approximated as follows: If we assume that individuals are fully rational and choose to travel through the off-ramp that minimises their travel time, then there exists an equilibrium point between exits A and B at which the travel time from both exits is identical. Suppose the velocity on the freeway is higher than that on the surface street network (i.e. $v_s < v_f$). In this case, the location of the equilibrium point can be determined using the following relationship.

$$d_f = d_1 + d_2$$
$$\frac{d_f}{v_f} + \frac{d_1}{v_s} = \frac{d_2}{v_s}$$

where d_f is the length between consecutive exits; d_1 and d_2 are distances to the equilibrium from exit A and exit B depicted in Fig. 2(a); v_f and v_s are speeds on the freeway and surface street networks respectively.

By solving the above equations simultaneously, the length of d_1 and d_2 can be obtained. For the original route (Fig. 2(a)), people with destinations below the equilibrium (in d_2) use exit A and people with destinations above the equilibrium (in d_1) use exit B. Therefore, $1 - v_s/(2v_f)$ proportion of people (in blue areas) exit through their nearest off-ramp and $v_s/(2v_f)$ proportion (in green area) exit through their second nearest off-ramp.

Similarly, considering that the intended exits are now missed (Fig. 2(b)), people living in the green area (the bottom segment) who previously travelled using exit A will now use exit B instead, which is their second order exit; people in the blue area (the middle segment) who previously used exit A now use exit B, their nearest exit; and people in the red zone (the top segment), who used exit B for travel now have to use the next downstream exit (not shown on the figure), which would be of order three. Therefore, after missing exits, $v_s/(2v_f)$ proportion of people use their nearest exit, $1/2$ proportion of them use the second nearest exit, and $1/2 - v_s/(2v_f)$ proportion use the third nearest exit.

Assuming that all segments between the exits follow the same allocation throughout the sample region, the representations for the mean D_F and D_S are:

$$\langle D_F \rangle = \frac{\sum_i^m d_{f,i}}{m} = \overline{d_f} \tag{1}$$

$$\begin{aligned} \langle D_S \rangle &= \overline{C}\left[\langle r_1 \rangle \frac{\overline{v_s}}{2\overline{v_f}} + \langle r_2 \rangle \frac{1}{2} + \langle r_3 \rangle \left(\frac{1}{2} - \frac{\overline{v_s}}{2\overline{v_f}}\right)\right] - \overline{C}\left[\langle r_1 \rangle \left(1 - \frac{\overline{v_s}}{2\overline{v_f}}\right) + \langle r_2 \rangle \frac{\overline{v_s}}{2\overline{v_f}}\right] \\ &= \overline{C}\left[\langle r_1 \rangle \left(\frac{\overline{v_s}}{\overline{v_f}} - 1\right) + \langle r_2 \rangle \left(\frac{1}{2} - \frac{\overline{v_s}}{2\overline{v_f}}\right) + \langle r_3 \rangle \left(\frac{1}{2} - \frac{\overline{v_s}}{2\overline{v_f}}\right)\right] \end{aligned} \tag{2}$$

where $d_{f,i}$ represents the distance of the ith gap between two successive exits; m is the total number of gaps between consecutive exits; $\overline{C}$ is the average circuity of the region; $\langle r_n \rangle$ is the average Euclidean distance between any random destination on the region and its nth closest exit; and $\overline{v_f}$ and $\overline{v_s}$ are the average speeds on freeway and street networks, respectively.

To estimate the average Euclidean distance from any destination to its nth closest exit $\langle r_n \rangle$, one can naively double-integrate the Euclidean norm for x over 0 to infinity and y from 0 to the height of the block. However, the solution does not converge to a finite value and, therefore, cannot be used for approximation. While it may be possible to numerically determine the range of y values, the resulting error would be too large for the approximation to be valid. Instead, we make the assumption that the spatial distribution of exits across the region follows a two-dimensional homogeneous Poisson point process (HPPP). This assumption allows us to generalise the problem and obtain a solution using probability theory. For a point process $\Phi \subset \mathbb{R}^2$ to be an HPPP, it has to inhere the following properties (Stoyan et al., 2013):

- The number of points of the point process Φ within any Borel set $B \subset \mathbb{R}^2$ follows a Poisson distribution, i.e.,

$$\mathbb{P}(\psi(B) = n) = \frac{e^{-\Lambda(B)}(\Lambda(B))^n}{n!} \tag{3}$$

  where $\psi(B)$ is the counting measure, defined as $\psi(B) = \sum_{x_i \in \Phi} \mathbb{1}(x_i \in B)$, and $\Lambda(B)$ is the intensity measure, defined as $\Lambda(B) = \mathbb{E}[\psi(B)]$.
- For M disjoint sets $B_1, \ldots, B_M$, the random variables $\psi(B_1), \ldots, \psi(B_M)$ are independent.
- The intensity λ is a constant.

A useful property that the HPPP exhibits for the derivation of the nth nearest neighbour distribution is motion-invariance (Daley and Vere-Jones, 2008). A point process is said to be motion-invariant if it is both stationary and isotropic. Stationary means that if the observer moves or translates the coordinate system, the distribution of the points do not change. Isotropic, on the other hand, implies that the distribution of points is invariant to the rotation of the axes. Together they suggest that regardless of the realisation of the subset B, the points inside will always follow the same HPPP (Poisson distributed with mean $\lambda\ell(B)$, where $\ell(B)$ is the area of B in $\mathbb{R}^2$). Consequently, the distributions of the nth nearest neighbours are invariant to the underlying distribution of the random destinations, such as homes, offices, and other functional areas, which are known to display heterogeneous spatial patterns. This property enables the modelling of exit-missing costs without making assumptions or evaluations on the spatial distribution of the destinations, which can simplify our analysis.

We now introduce the cumulative distribution function (CDF) and the probability density function (PDF) for the distance R_n to the nth nearest point from the origin. This is an extension to the distance distribution of the nearest neighbour commonly used in wireless communication problems (Baccelli et al., 1997).

Lemma 1. *The CDF and PDF of the nth nearest-neighbour distance for a motion-invariant HPPP Φ with intensity λ are*

$$CDF: F_{R_n}(r_n) = 1 - e^{-\lambda\pi r_n^2} \sum_{k=0}^{n-1} \frac{(\lambda\pi r_n^2)^k}{k!} \tag{4}$$

$$PDF: f_{R_n}(r_n) = \frac{e^{-\lambda\pi r_n^2}(\lambda\pi r_n^2)^{n-1}}{(n-1)!} 2\lambda\pi r_n \tag{5}$$

Proof. By definition, the CDF of R_n is

$$F_{R_n}(r_n) = \mathbb{P}(R_n \le r_n) = 1 - \mathbb{P}(R_n > r_n)$$

Envisage a disk $B(o, r_n)$ with its centre at the origin and radius r_n. The event that the distance of the nth closest point R_n is greater than r_n implies that the number of points intersecting the disk would be at most $n-1$. Thus, the above expression can be elaborated as follows

$$F_{R_n}(r_n) = 1 - \mathbb{P}(\psi(B(o, r_n)) \le n-1) = 1 - \sum_{k=0}^{n-1} \mathbb{P}(\psi(B(o, r_n)) = k)$$

We know from the definition that $\psi(B(o, r_n))$ is Poisson distributed. Therefore, the CDF of R_n is given by

$$F_{R_n}(r_n) = 1 - \sum_{k=0}^{n-1} \frac{e^{-\lambda\pi r_n^2}(\lambda\pi r_n^2)^k}{k!}$$

Then, the PDF of R_n is simply obtained by differentiating the CDF with respect to r_n. Or else, the PDF can be derived by calculating the product of the probabilities that $n-1$ points are embedded in the disk and 1 point lies on the disk. Both would yield the same function. □

From this point, the average distance to the nth closest point can be computed as

$$\langle r_n \rangle = \frac{\int_0^\infty r_n f(r_n) \mathrm{d}r_n}{\int_0^\infty f(r_n) \mathrm{d}r_n} = \frac{\int_0^\infty r_n e^{-\lambda\pi r_n^2}(\lambda\pi r_n^2)^{n-1} 2\pi r_n \lambda \, \mathrm{d}r_n}{\int_0^\infty e^{-\lambda\pi r_n^2}(\lambda\pi r_n^2)^{n-1} 2\pi r_n \lambda \, \mathrm{d}r_n} \tag{6}$$

By substituting $\lambda\pi r^2$ with u, we can determine the mean cost as follows:

$$\langle r_n \rangle = (\lambda\pi)^{-\frac{1}{2}} \frac{\int_0^\infty e^{-u} u^{n-\frac{1}{2}} \, \mathrm{d}u}{\int_0^\infty e^{-u} u^{n-1} \, \mathrm{d}u} = (\lambda\pi)^{-\frac{1}{2}} \left[\frac{\Gamma(n+\frac{1}{2})}{\Gamma(n)} \right] \tag{7}$$

With the above derivations, the average distance cost for missing exits can be approximated:

$$\langle D\rangle = \overline{d}_{\mathrm{f}} + \frac{\overline{C}}{\sqrt{\lambda\pi}}\left[\left(\frac{\overline{v}_{\mathrm{s}}}{\overline{v}_{\mathrm{f}}} - 1\right)\left(\Gamma(1.5) - \frac{\Gamma(2.5)}{2} - \frac{\Gamma(3.5)}{4}\right)\right] = \overline{d}_{\mathrm{f}} + \frac{11\overline{C}}{32\sqrt{\lambda}}\left[1 - \frac{\overline{v}_{\mathrm{s}}}{\overline{v}_{\mathrm{f}}}\right] \tag{8}$$

The time cost can also be approximated using the solution we derived above. By considering the distance cost on the freeway and surface street separately, the approximated time cost is

$$\begin{aligned}\langle T\rangle &= \frac{\langle D_{\mathrm{F}}\rangle}{\overline{v}_{\mathrm{f}}} + \frac{\langle D_{\mathrm{S}}\rangle}{\overline{v}_{\mathrm{s}}}\\ &= \frac{\overline{d}_{\mathrm{f}}}{\overline{v}_{\mathrm{f}}} + \frac{\overline{C}}{\overline{v}_{\mathrm{s}}\sqrt{\lambda\pi}}\left[\left(\frac{\overline{v}_{\mathrm{s}}}{\overline{v}_{\mathrm{f}}} - 1\right)\left(\Gamma(1.5) - \frac{\Gamma(2.5)}{2} - \frac{\Gamma(3.5)}{4}\right)\right] = \frac{\overline{d}_{\mathrm{f}}}{\overline{v}_{\mathrm{f}}} + \frac{11\overline{C}}{32\sqrt{\lambda}}\left[\frac{1}{\overline{v}_{\mathrm{s}}} - \frac{1}{\overline{v}_{\mathrm{f}}}\right]\end{aligned} \tag{9}$$

2.2. Standard deviation of exit-missing costs

To fully characterise the exit-missing cost, we also formulate the standard deviation of the costs. The cost functions consist of a number of random variables, including the exit gap (d_{f}), circuity (C), freeway speed (v_{f}), surface street speed (v_{s}), as well as the Euclidean distance to the three nearest exits (r_1, r_2, r_3). The standard deviation of the costs can be determined by considering the variance of each random variable and their respective covariance. Note, the parameter λ is implicitly considered in the mean distance to the nearest neighbours (r_1, r_2, r_3).

We approximate the variance of the cost functions using the Delta method (Liu, 2012). Here, we assume all variables are independent, and the covariance terms are zero. Note the Euclidean distance to the three nearest exits (r_1, r_2, r_3) are assumed to be independent because these distances are calculated from any random points in the region where the variables are three independent realisations of the same underlying point process. First, we confirm that both the distance and time cost functions are smooth (i.e. continuous and differentiable), which indicates that they can be approximated with Taylor expansion. To avoid an infinite regress of higher-order terms, we use the first-degree Taylor polynomial around the population mean μ. A function g with k independent random variables is expressed as:

$$g(x_1,\ldots,x_k) \cong g(\mu_1,\ldots,\mu_k) + (x_1-\mu_1,\ldots,x_k-\mu_k)\begin{pmatrix}\frac{\partial g}{\partial x_1}(\mu_1,\ldots,\mu_k)\\ \vdots\\ \frac{\partial g}{\partial x_k}(\mu_1,\ldots,\mu_k)\end{pmatrix} \tag{10}$$

To use the Delta method for approximating the underlying distribution of function g, we assume all variables are asymptotically normal (i.e., $x_i \sim N(\mu_i, \sigma_i^2)$ for large samples). This is a reasonable assumption and allows us to avoid other assumptions for the back-transformation. Moreover, this assumption leads to reasonable estimates of mean and variance, as shown later in Section 3.2. After rearrangement, $x_i - \mu_i \sim N(0, \sigma_i^2)$. Therefore:

$$(g(x_1,\ldots,x_k) - g(\mu_1,\ldots,\mu_k)) \cong (N(0,\sigma_1^2),\ldots,N(0,\sigma_k^2))\begin{pmatrix}\frac{\partial g}{\partial x_1}(\mu_1,\ldots,\mu_k)\\ \vdots\\ \frac{\partial g}{\partial x_k}(\mu_1,\ldots,\mu_k)\end{pmatrix} \tag{11}$$

Hence, by the properties of the normal distribution:

$$g(x_1,\ldots,x_k) \sim N\left(g(\mu_1,\ldots,\mu_k), (\sigma_1^2,\ldots,\sigma_k^2)\begin{pmatrix}\left(\frac{\partial g}{\partial x_1}(\mu_1,\ldots,\mu_k)\right)^2\\ \vdots\\ \left(\frac{\partial g}{\partial x_k}(\mu_1,\ldots,\mu_k)\right)^2\end{pmatrix}\right) \tag{12}$$

To adapt the above expression to our problem, the partial derivatives of the variables for both the time and distance costs are obtained and summarised in Table 1.

An estimation of the variance for the exit gaps, circuity, freeway speed, and surface street speed can all be obtained numerically, whereas the variance ($\sigma_{r_n}^2$) of the distance r_n to the nth nearest exit requires the formulation of its mean (Eq. (7)) and the second statistical moment of the probability density:

$$\begin{aligned}\sigma_{r_n}^2 &= \mathbb{E}(r_n^2) - (\mathbb{E}(r_n))^2\\ &= \frac{\int_0^\infty r_n^2 e^{-\lambda\pi r_n^2}(\lambda\pi r_n^2)^{n-1}2\pi r_n\lambda\,\mathrm{d}r_n}{\int_0^\infty e^{-\lambda\pi r_n^2}(\lambda\pi r_n^2)^{n-1}2\pi r_n\lambda\,\mathrm{d}r_n} - (\lambda\pi)^{-1}\left(\frac{\Gamma(n+\frac{1}{2})}{\Gamma(n)}\right)^2\\ &= (\lambda\pi)^{-1}\left(\frac{\Gamma(n+1)}{\Gamma(n)}\right) - (\lambda\pi)^{-1}\left(\frac{\Gamma(n+\frac{1}{2})}{\Gamma(n)}\right)^2\\ &= (\lambda\pi)^{-1}\left[n - \left(\frac{\Gamma(n+\frac{1}{2})}{\Gamma(n)}\right)^2\right]\end{aligned} \tag{13}$$

Table 1
Partial derivatives for all random variables in the cost functions.

	Distance cost (D)	Time cost (T)
$\frac{\partial}{\partial d_f}$	1	$\frac{1}{v_f}$
$\frac{\partial}{\partial C}$	$r_1\left(\frac{v_s}{v_f}-1\right)+r_2\left(\frac{1}{2}-\frac{v_s}{2v_f}\right)+r_3\left(\frac{1}{2}-\frac{v_s}{2v_f}\right)$	$r_1\left(\frac{1}{v_f}-\frac{1}{v_s}\right)+r_2\left(\frac{1}{2v_s}-\frac{1}{2v_f}\right)+r_3\left(\frac{1}{2v_s}-\frac{1}{2v_f}\right)$
$\frac{\partial}{\partial v_f}$	$C\left[-r_1\frac{v_s}{v_f^2}+r_2\frac{v_s}{2v_f^2}+r_3\frac{v_s}{2v_f^2}\right]$	$-\frac{d_f}{v_f^2}+C\left[-r_1\frac{1}{v_f^2}+r_2\frac{1}{2v_f^2}+r_3\frac{1}{2v_f^2}\right]$
$\frac{\partial}{\partial v_s}$	$C\left[\frac{r_1}{v_f}-\frac{r_2}{2v_f}-\frac{r_3}{2v_f}\right]$	$C\left[\frac{r_1}{v_s^2}-\frac{r_2}{2v_s^2}-\frac{r_3}{2v_s^2}\right]$
$\frac{\partial}{\partial r_1}$	$C\left(\frac{v_s}{v_f}-1\right)$	$C\left(\frac{1}{v_f}-\frac{1}{v_s}\right)$
$\frac{\partial}{\partial r_2}$	$C\left(\frac{1}{2}-\frac{v_s}{2v_f}\right)$	$C\left(\frac{1}{2v_s}-\frac{1}{2v_f}\right)$
$\frac{\partial}{\partial r_3}$	$C\left(\frac{1}{2}-\frac{v_s}{2v_f}\right)$	$C\left(\frac{1}{2v_s}-\frac{1}{2v_f}\right)$

Therefore, for a cost function g (either D or T), the estimated standard deviation is calculated as follows:

$$\hat{\sigma_g} = \sqrt{\sum_{x\in\{d_f,C,v_f,v_s,r_1,r_2,r_3\}} \left(\frac{\partial g(\overline{d_f},\overline{C},\overline{v_f},\overline{v_s},\langle r_1\rangle,\langle r_2\rangle,\langle r_3\rangle)}{\partial x}\right)^2 \sigma_x^2} \tag{14}$$

3. Simulation experiments of exit-missing costs in the top 50 metropolitan areas

While we have formulated the exit-missing costs analytically, their performance against the actual values is as yet undetermined. Since real GPS data containing missed exits are rare (we discuss an example in a subsequent section), we evaluate our model with simulated costs for the 50 most populated metro areas in the US. The effectiveness of the model is showcased against a baseline, and various evaluation metrics are calculated. The limitations of the analytical model are discussed in Section 5.

3.1. Extraction of exit-missing costs

This section demonstrates the computations of exit-missing costs for the top 50 most populated metro areas in the US. All trips involving links outside of the metros are discarded. The trip generation data used in our research is a subset of the 2013 Longitudinal Employer-Household Dynamics (LEHD) dataset termed LEHD Origin–Destination Employment Statistics (LODES), which contains state-wise commuting data at census block levels (US Census Bureau, 2022a). A census block is the smallest areal unit for which detailed social demographic and mode share data are available. A typical census block consists of 250–550 housing units, and for this reason, the inter-block commuting number is usually small (most are 0 or 1).

The shapefiles of these census blocks were acquired from the Census TIGER/line files (US Census Bureau, 2022b). Since not all centroids lie within their respective blocks, the internal points of the polygons are snapped to their nearest nodes in the 2013 Open Street Map (OSM) traffic network. One drawback of the OSM network is the absence of speed limits on some links. This was accounted for by imputing the travel speeds of the missing values using the mean of the remaining links for the particular highway type. The link travel time is then calculated using the speed and the length. It should be noted that we have omitted the impact of traffic congestion in this Section; the travel time calculated is based solely on the free-flow speed. The impact of traffic congestion on exit-missing costs is further evaluated in Section 4.2.4.

The method we use to determine the exit-missing costs is by randomly sampling 10,000 OD pairs from the LODES data for each metropolitan area, where the sampling weight follows from the inter-block commuting number (i.e. the number of trips belonging to an OD). For the sake of simplicity, we assume all flows on an OD pair are allocated to the shortest path according to an all-or-nothing assignment. Then for each OD, Dijkstra's algorithm computes the shortest path with travel time as the edge impedance. This route is then regarded as the original route with its final exit stored (if it exists, else remove the OD from the list). The travel costs, namely time and distance, from the upstream point of the final exit to the destination are computed as the original costs. The alternative path assumes the driver has missed the intended exit and will use the following off-ramp to exit the freeway, that is of saying, the alternative route proceeds along the mainline, and the shortest path algorithm is utilised to determine the most efficient route from the second exit to the destination. The travel costs for this shortest path, along with the extra portion on the freeway, are calculated as the alternative costs. Consequently, the cost of missing an exit is calculated by subtracting the original cost from the alternative cost. Since both routes are computed from the shortest paths, the cost is guaranteed to be positive. Finally, for each metro area, the costs from all the sampled ODs are aggregated across the commuting population, and the mean and standard deviation of the costs are computed. Note that the impacts of traffic flows, variations in speed, and the presence of traffic signals are not accounted for in this section. To overcome the above limitations, we conduct experiments on a real-world GPS dataset in Section 4. The LEHD dataset used in this section only contains commuting OD information. Further commuting related analysis are also investigated in Section 4. The empirical results demonstrate that the exit-missing costs are consistent with the values computed in this section and thus support the conclusion that costs for missed exits are negligible.

3.2. Goodness of fit with analytical costs

We undertake a comparative analysis to showcase the dependencies between predicted and observed costs. Fig. 3 illustrates the scatter plots of the simulated mean values and the estimated mean values of the distance and time costs of missing the freeway exit. Likewise, residual plots are presented to showcase potential bias in our model. Residuals are calculated by subtracting the predicted values from the actual/simulated values. The scatter plots show a clear linear relationship between the two variables for both time and distance, and the points scatter approximately along the 45-degree line. Las Vegas (LAS), Riverside (RAL), and Salt Lake City (SLC) are exceptions that are computed to be outliers using the Bonferroni outlier test (Fox, 2008). Further looking into the three instances shows that the low exit densities, together with large exit gaps, have contributed to the large discrepancies. As an example, the average exit gap for SLC is 4.380 km, which even exceeds the total predicted distance costs (average exit gap and surface street network cost combined) for most metro areas. This is due to extremely large exit gaps embedded in the metropolitan regions (maximum gap length of 68.470 km for SLC), which inflate the average gap length. Moreover, the three outliers have the lowest exit densities among all 50 metros. This is due to them having dispersed freeway networks, lowering the exit-area ratio, and further exaggerating the costs. Thus, it is reasonable to conjecture that the models would align more closely in regions where freeway exits exhibit more uniform densities. In urban settings, freeways and their exits tend to be densely distributed, whereas inter-urban freeways and their exits are sparser. When considering the metropolitan region in its entirety, there will be zones with denser exits and others that are less dense. This variability likely accounts for the significant discrepancies observed in the predicted values.

The root-mean-square error (RMSE) and mean absolute error (MAE) are applied as the evaluation metrics for quantifying the performance of the predicted costs. After removing the outliers, namely SLC, RAL, and LAS, the RMSE and MAE for distance costs are 0.524 km and 0.413 km, respectively. While for the time costs, the RMSE and MAE are 0.418 min and 0.333 min. To extrapolate what these figures suggest, we construct a simple baseline for the predictor using the mean of the 50 observed values (3.558 km for distance and 2.307 min for time). The respective RMSE and MAE for distance costs are 0.831 km and 0.716 km, and for time are 0.465 min and 0.392 min. Hence, our model has outperformed the simple baseline model with solely the information on metropolitan road networks and can thus provide valuable insights into the compositions of the costs.

In addition, we conducted a stratified analysis of the simulated costs, distinguishing between trips made to work and those made returning home, and assessed the model's performance in each case. The scatter diagrams for the two scenarios are illustrated in Fig. 4. Notably, the MAE values indicate that the model performs better for the to-home trips than the to-work trips. This is because our model is formed based on the assumption that the exits are distributed homogeneously, implying that analytical outcomes remain constant irrespective of destination distribution (due to motion-invariance). However, in reality, the exits are not distributed homogeneously, and neither are the destinations. While setting the destinations to homes does not make the exits appear homogeneous, the simulated relative spacings between the two would be more homogeneous since homes are more widely located than workplaces, which are more often concentrated in business districts. If the distribution of the destinations is highly clustered or regular in the vicinity of the exit points, then the travel distance between the two sets may be affected by this inhomogeneous nature of the destination set.

The results for the standard deviation of the costs are somewhat less promising (shown in Fig. 5). Although there is still a positive correlation between the predicted and observed values, the analytical model tends to produce underestimated standard deviations, as shown by the points falling in the lower half of the scatter plot and the residuals clustering at some positive values. The reason behind this discrepancy is twofold. First and foremost, we assume the distribution of exits to be spatially homogeneous, which would down-estimate the variance for the distance to the nth closest exits. Secondly, we assume that the random variables in the formulations are independent, which yields zero covariance between the terms. However, in reality, many of these variables, such as the exit gap length and the distance to the nth nearest exit, are interdependent. As a result, the variance and hence the standard deviation of the costs are undervalued. One outlier has been detected for both the distance and the time costs, which is Salt Lake City. The much higher than rest variance for the exit gap length ($\sigma^2_{d_f}$ = 64.007 km^2) and the distance to exits ($\sigma^2_{r_1}$ = 9.483 km^2; $\sigma^2_{r_2}$ = 10.290 km^2; $\sigma^2_{r_3}$ = 10.554 km^2) led to this abnormality. Apart from SLC, the standard deviation of many other metro areas also diverge from the dominant stream. The reasoning is more or less the same: metros with fewer off-ramps have high variation in exit gap length and distance to the nearest exits, which consequently overstates the variance of the functions.

In line with the evaluation of the mean, the RMSE and MAE measures are applied to the predicted standard deviation of the costs. The RMSE and MAE for the standard deviation of the distance costs are 1.257 km and 1.055 km, and are 0.741 min and 0.614 min for time costs. The means of the 50 observed standard deviations are again used as the baseline. The RMSE and MAE for the baseline are computed to be 1.133 km and 0.938 km for distance costs, and 0.628 min and 0.492 min for time costs. This implies that our model underperformed against the baseline. However, the model performance is reasonable, considering that only network variables are fed into the model and that the dispersion of data around the mean is typically harder to predict. Since we have already assessed the impact of the normality assumption on the predictions, it is unlikely that the observed discrepancies stem from this specific assumption. Instead, we suspect the large discrepancy arises from assuming the variables are independent. Without knowledge of the asymptotic distributions of these variables, determining their covariances is challenging. By assuming the variables are independent, only the variance matrix is needed in the calculations. Since we want to find the within-metropolitan variances of the travel costs, it is essential to determine the within-metropolitan covariances of the variables. However, given that the variables were not sampled concurrently and have distinct contexts (e.g., speed was derived from road links, while circuity was obtained from simulated trips), it is infeasible to compute their covariance. Thus, to quantify the joint variability between these variables, their joint distributions would be necessary, but this information is absent. Consequently, future research should aim to

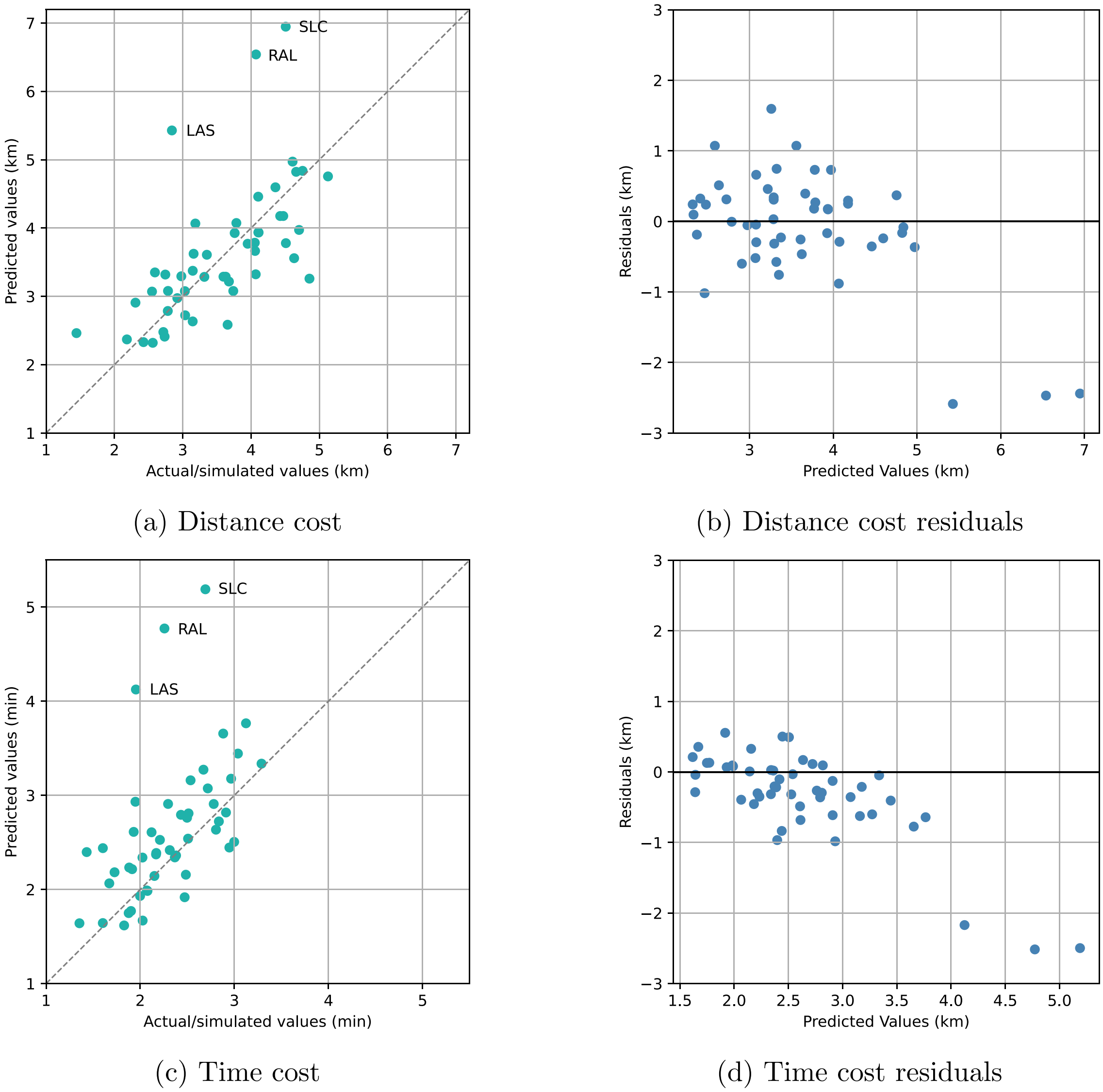

Fig. 3. Scatter plots comparing the actual and predicted mean of costs. Subplots (a) and (c) are scatter plots showing the relationship between the observed and predicted values. The three outliers marked are Las Vegas (LAS), Riverside (RAL), and Salt Lake City (SLC). Subplots (b) and (d) are residual plots showcasing the distribution of residuals against the predictions. The MAE for the exit-missing distance cost is 0.413 km, and is 0.333 min for the exit-missing time cost.

identify and quantify the joint variability between these variables and assess if this contributes to the disparity between predicted and simulated values.

Finally, it is crucial to highlight that the residuals in Figs. 3(b) and 3(d), as well as Figs. 5(b) and 5(d), seem to be non-normally distributed. In fact, the error is decreasing with increasing predicted values. This pattern is likely a result of the inhomogeneous distributions of the exits. Given our HPPP assumption, the analytical model exhibits a strong dependence on the distribution of off-ramps from the networks. The considerable variability in exit density and exit gap length leads the predictions to overshoot the actual values in regions with vast area but sparsely populated off-ramps. This model limitation is elaborated upon in the limitations in Section 5.

4. Empirical evidence for exit missing costs

In this section, we analyse GPS datasets to corroborate our prior conclusions that the costs associated with missing off-ramps are not excessively high. Due to the scarcity of real-time vehicle data, our analysis is limited to a single metro area out of the 50 metro areas we have covered. Specifically, we focus our investigation on the Minneapolis-St. Paul metropolitan area. Since the LODES dataset only provides commuting OD information, our analysis in this section encompasses both commuting and non-commuting

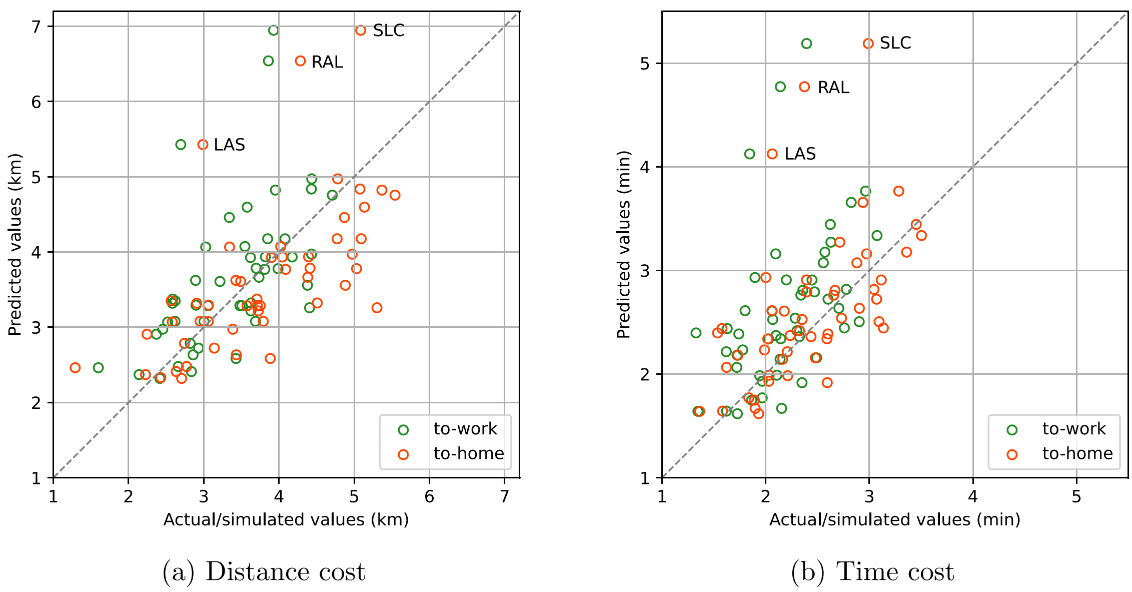

Fig. 4. Scatter plots for the actual and predicted mean of costs for to-work and to-home trips. To-work trips are shown in green and to-home trips are in red. The outliers marked are Las Vegas (LAS), Riverside (RAL), and Salt Lake City (SLC). Subplots (a) and (b) illustrate the scatters of the distance and time costs, respectively. The MAE for the exit-missing distance cost for the respective to-work and to-home trips are 0.438 km and 0.531 km. For the exit-missing time cost, the MAE for the respective to-work and to home trips are 0.414 min and 0.313 min. (For interpretation of the references to colour in this figure legend, the reader is referred to the web version of this article.)

trips, intending to identify any disparities in their cost distributions. The relationship between peak hour congestion and exit-missing costs is likewise assessed. Apart from the evaluation of time and distance costs, we also incorporate the computation of circuity and a deviation measure, which serves to quantify the spatial dissimilarity between the two routes. These measurements help us explore the consequences of missing freeway off-ramps and are discussed in Appendix C. Furthermore, in Appendix D, we conduct a categorical analysis on the exiting behaviours detected in the two datasets. A simple heuristic is introduced to extract trips that possibly missed their intended off-ramps.

Below, we set out a list of hypotheses that are of interest to our study:

1. Missing freeway exits will incur additional travel time and distance. However, from the results in Section 3.2, we hypothesise that the exit-missing costs are low (only a matter of minutes for time and kilometres for distance);
2. The cost distribution of missing an exit for commuting trips and non-commuting trips are not significantly different from the supply/network perspective;
3. The costs for missing exits depend on the traffic conditions. In peak hour periods, we presume the costs are more severe, especially for the time cost, since congestion may further delay the travel time;
4. There exists a positive relationship between deviation and exit-missing costs. The larger the deviation (spatial dissimilarity) between the original and alternative routes, the higher the additional travel time or distance (discussed in Appendix C);
5. The mean circuitousness of alternate routes is anticipated to surpass that of the original routes due to excess rerouting (discussed in Appendix C);

4.1. Method for empirical analysis

4.1.1. Datasets and pre-processing

Two datasets were employed in our study: the I-35W dataset and the Travel Behaviour Inventory (TBI) dataset. The I-35W data were collected for part of a traffic behaviour research on the resilience of traffic systems when a detrimental event occurs, in this case before and after the reopening of the I-35W Mississippi River Bridge, which collapsed in 2007 (Zhu et al., 2010). The GPS data were collected for up to 13 weeks in 2008/2009. The participants were required to install either a logging device (Otrec) or a real-time communication device (VMT) on their cars. Out of 190 subjects who participated, 143 records were retrieved and utilised for our study. 47 of them (VMT) were recorded using an installed GPS unit with a frequency of one point per second, while the rest 96 (Otrec) were recorded using a portable GPS unit plugged into an in-vehicle power source, with a frequency of one point every 25 m.

The TBI dataset was collected in 2010/2011 by the Metropolitan Council of the Twin Cities. GPS devices were deployed to 278 individuals from 250 households, who carried them on their person for all of their travel, including both in and outside of cars. Consequently, prior to undertaking other pre-processing procedures, the TBI data necessitated trip stratification, mode classification,

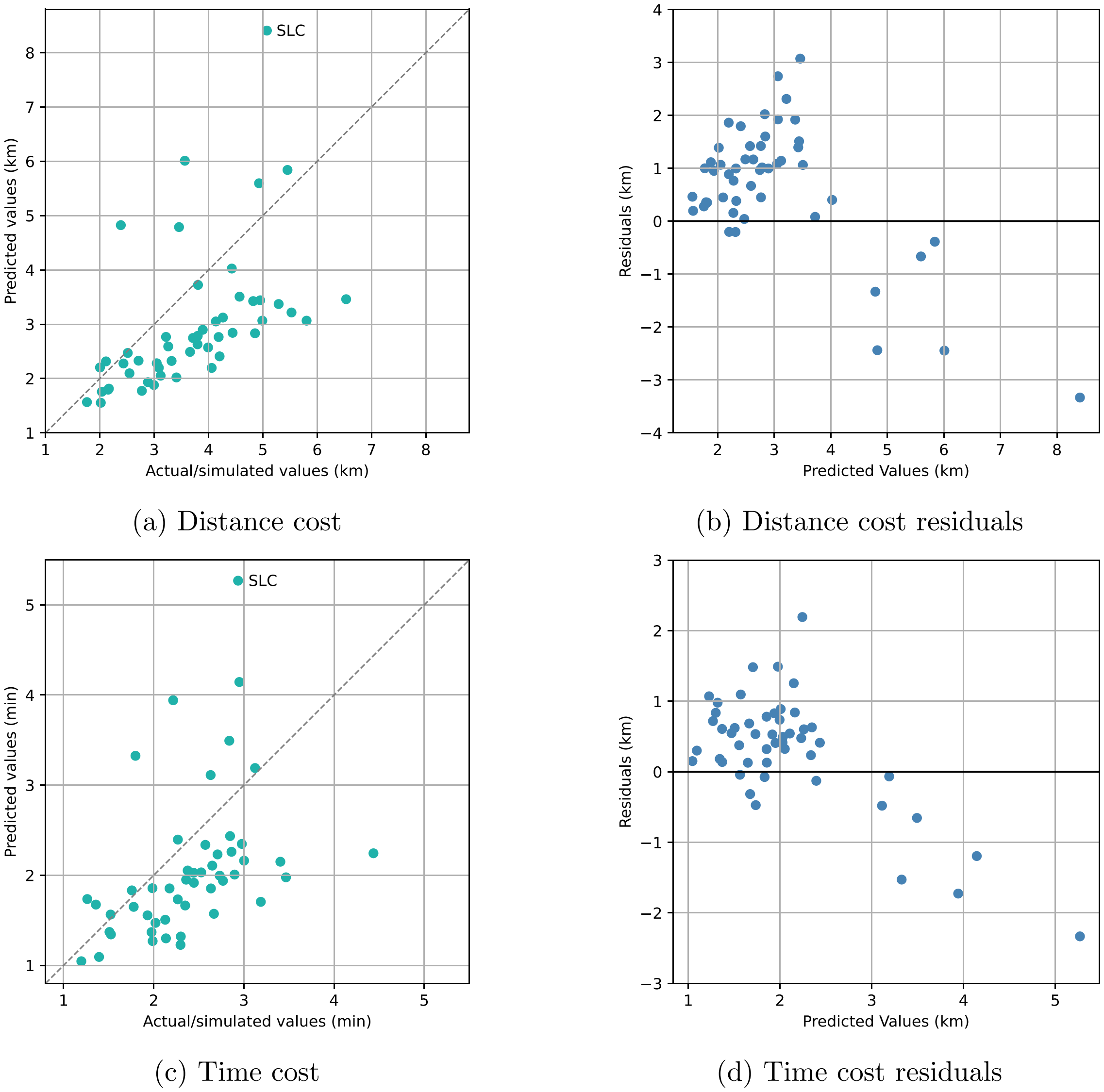

Fig. 5. Scatter plots for the actual and predicted standard deviation of costs. Subplots (a) and (c) are scatter plots showing the relationship between the observed and predicted values. The outlier marked represents Salt Lake City (SLC). Subplots (b) and (d) are residual plots showcasing the distribution of residuals against the predictions. The MAE for the standard deviation of exit-missing distance cost is 1.055 km, and is 0.614 min for the standard deviation of exit-missing time cost.

and trip purpose identification. We modified the simple set of rules designed by Tang and Levinson (2018) to perform the above three tasks. The mode identification process is based on studies by Chen et al. (2010), Gong et al. (2012). The trips were first stratified by placing a 300-s threshold on the time gaps of successive GPS points. Then, the car mode was classified with the following rules:

- Average speed of all points > 10 km/h, which precludes most walking trips.
- Maximum speed of all points > 30 km/h, which precludes most cycling trips.
- If both the first and last points with speed ≥ 10 km/h lie within 50 m of bus stops, the trip is considered in bus mode and removed.
- If both the first and last points with speed ≥ 10 km/h lie within 150 m of rail stations, the trip is considered in rail mode and removed.

Finally, trip purposes are identified by matching the relative location of origin and destination with the known home and work location of the subject. A 500-m buffer region is used to account for parking and GPS error. The applied process exclusively identifies car trips, wherein these trips are subsequently classified into either commuting or non-commuting categories.

Table 2
Summary of the data pre-processing steps. VMT and Otrec together contribute to the I-35 W dataset. For each dataset, both the numbers of trips and points are showcased, as well as the original and final data size. The Otrec data do not contain speed attributes; thus, the speed filter is omitted.

	VMT		Otrec		TBI	
	Trips	Points	Trips	Points	Trips	Points
Original	32,730	18,334,840	16,658	7,344,553	3,470	8,721,622
Warm/cold start	−3,906	−3,500,813	−637	−512,852	−198	−3,841,283
Boundary elimination	−730	−1,001,889	−7	−4,654	−192	−969,389
Short trips	−13,630	−413,854	−2,046	−105,458	−117	−6,102
Position jump	0	−937	0	−964	0	−53
Abnormal speed	0	−169,272	–	–	0	−3,879
Fill missing	0	+170,653	0	+698	0	+340,538
Circuity	−1,653	−2,492,702	−1,191	−542,778	−296	−922,571
Final	12,811	10,926,026	12,777	6,178,545	2,667	3,318,883

Although the datasets are of high resolution, some data-cleaning steps are still necessary. The data first undergo filtering to eliminate a set of beginning and ending points to address the so-called warm-start-cold-start problem and the excess dwell time at the destination. A trip is updated with its new origin, the first point with distance from the original origin ≥ 50 m, and the updated destination, the first point with distance from the original destination ≤ 50 m. Afterwards, a rough location screening is performed by fitting the trips to the Twin Cities region. In addition, we address potential positional jumps in the data by incorporating a small elliptical zone for each GPS point using their respective coordinate, speed, heading, and a 50 m error buffer. Points outside their neighbours' zones are recognised as off-route points and removed. Abnormal speed changes, defined with an instantaneous acceleration of ± 5 m s^{-2}, are also identified and removed from the data. Another common type of speed anomaly, caused by the interference of the satellite signals, usually emerges in the form of a sudden drop of velocity to zero along with linearised trajectory points. These points are likewise removed by tracking the speed change of the vehicles and identifying obstructions, primarily tunnels, in the network. Finally, the missing gaps are filled with interpolated points to construct continuous, connected trips.

Furthermore, we preclude detour routes which may cause misleading outputs. Such excess routing may be undertaken to facilitate the pick-up or drop-off of passengers, resulting in original travel expenses that are well beyond the shortest path costs. Hence, the alternative route computed by the shortest path algorithm can have substantially shorter travel costs than the original route, leading to savings in time and distance by missing an exit. In response, we apply the network circuity to remove trips based on their directness. The top 10th percentile of all trips is removed with an upper bound threshold of 1.84 for the I-35W dataset and 2.25 for the TBI dataset.

Finally, the processed trips are matched with the 2013 OSM network, the earliest and most compatible open-source map regarding the data collection time frame. As one of the test variables for the dataset, the I-35W bridge is removed from the network before the reopening date of 18th September 2008. The map-matching algorithm employed was developed using the hidden Markov model and a set of precomputed shortest paths (Yang and Gidófalvi, 2018). This algorithm takes into account connectivity and adjacency between consecutive points. The links included in the precomputation were within 3 km from the points, thus significantly increasing the computational speed of the matching process when querying from the database.

The above procedure is applied to I-35W and TBI datasets with the carry-over data analysed to test the hypotheses. Table 2 summarises trips and points removed in each pre-processing step.

4.1.2. Estimation of exit-missing costs

To compute the travel time on specific links, we utilise the TomTom Twin Cities dataset, which contains link-wise speed information from 2010 that has been preserved in databases categorised by the time of day. These data attributes are transferred to the high-resolution OSM network, which had previously been employed for map-matching purposes. Due to the mismatching links for the two road networks, we assign the speed attributes through the largest overlapping proportion between the TomTom network and an auxiliary OSM buffer. The match yields a 95.9% coverage, which implies that only 4.1% of the OSM network is not adapted with a link speed. These remaining links mainly comprise minor local roads, and their speeds are extrapolated using the mean of the three nearest neighbouring edges. To provide a fair comparison between the intended trajectory and the best alternative, we calculate the trip travel times based solely on the network edges matched to the GPS points. It should be noted that the TomTom network takes into account factors such as turns, congestion, and traffic signals implicitly in its speed data. Moreover, we make the assumption that drivers travel at the median (50th percentile) speed for their respective time of day.

The approach of finding the exit-missing costs is similar to that introduced in Section 3.1. Based on the GPS dataset and road network, we identify the freeway off-ramps the participants used to exit freeways. To mimic the behaviour of missing an exit, Dijkstra's algorithm is then performed from the source node of the second exit to the final point mapped to the network. Link impedances for shortest path calculations are based on the travel time of each link, which is estimated using the link length divided by the TomTom link speed. The shortest path from the second exit, together with the additional segment on the freeway, constitute the alternative route. Time and distance differences between the original route and its alternative are used to quantify the costs of missing exit.

Table 3
Number of exits extracted from datasets. VMT and Otrec together contribute to the I-35 W dataset.

	Final		Interim		All	
	Commute	Non-commute	Commute	Non-commute	Commute	Non-commute
VMT	934	5,282	723	3,861	1,657	9,143
Otrec	1,777	4,336	1,486	3,370	3,263	7,706
TBI	177	1,063	137	1,026	314	2,089

Table 4
Summary of the time cost of missing exits. (** $p \leq 0.01$, * $p \leq 0.05$).

		I-35W		TBI	
		Without SP constraint	With SP constraint	Without SP constraint	With SP constraint
All exits	Mean (min)	0.479	1.612	0.163	1.833
	Median (min)	1	2	1	2
	Std (min)	2.931	1.704	4.129	1.683
	Min (min)	−24	−8	−49	−31
	Max (min)	14	14	12	12
	Sample size	21,769	15,727	2,403	1,625
	p-value	0.000e−30**	0.000e−30**	0.027*	0.000e−30**
Final exits	Mean (min)	0.636	1.808	0.275	1.894
	Median (min)	1	2	1	2
	Std (min)	2.824	1.631	3.161	1.642
	Min (min)	−23	−3	−24	−1
	Max (min)	14	14	12	12
	Sample size	12,329	7,936	1,240	715
	p-value	0.000e−30**	0.000e−30**	1.118e−3**	0.000e−30**

4.2. Empirical results

This section presents the empirical results from I-35W and TBI datasets and provides a comprehensive discussion of the attributes of exiting activities. Our empirical analysis indicates that the costs associated with missing exits are consistent with the analytical and simulated values we have obtained. Collectively, these findings suggest that the exit-missing costs are on the order of a few minutes or kilometres. The number of outputted samples from the two empirical datasets are summarised in Table 3. A total of 24,002 exiting behaviours are observed, and the spatial distribution of these exits is illustrated in Appendix B.

4.2.1. Costs of missing exit

We start by discussing whether missing exits incur additional travel costs for drivers and, if so, how costly missing exits are. Costs are evaluated in terms of additional time and distance from the difference between the original route and its alternative. Computation of the costs is discussed in Section 4.1.2. We analyse two scenarios in this study. The first comprises all exits used by the drivers. This approach can be somewhat biased since a human-chosen route (original) is compared with a shortest time path (alternative), which may result in considerably large time/distance savings (negative costs) when an exit is missed. Therefore, we adopt another scenario (named with SP constraint hereafter), which consists of exits with their remaining portion of the trip (from the upstream node of CE to the destination) within 10% of the shortest path travel time. By applying the shortest path filter, we are able to ensure that the original and alternative routes are comparable.

Fig. 6 presents distributions of the time costs of missing exits for exits in I-35W and TBI datasets. Two exiting scenarios are showcased for the costs. The first includes all exits within each trip, which consists of both final and interim exits. The second scenario involves only the final exits of each trip. From Fig. 6, density plots without the SP constraint all exhibit left skewness, indicating that a significant proportion of the trips deviate from the shortest path to such an extent that the variation is even greater than that resulting from a missed exit. This has an adverse effect on the accuracy of our analysis and justifies the introduction of the shortest path filter. However, even without the SP constraint, both the mean and the median of all four cases still lie above 0. Table 4 summarises the statistics for distributions of the time cost of missing exits and their respective *p*-values. Here we applied the one-sample t-test with the null hypothesis: the mean of the additional travel time from missing exits is less than or equal to 0. All *p*-values are statistically significant, which provides evidence for us to reject the null hypothesis in favour of its alternative. Although we confirm missing an exit does incur additional travel time, the magnitude of the increase is generally mild.

Moreover, we compare the empirically derived results with those from our analytical derivations and simulations. To maintain consistency, only the final exits are considered in the comparison. Combining the I-35W and TBI samples yields a mean of 1.815 min and a standard deviation of 1.632 min. Based on the combined mean, there are, respectively, 9% and 14% over-estimations for the analytical and simulated results (1.984 min and 2.077 min). Similarly, the combined standard deviations is compared to the analytical and simulated values (1.472 min and 2.019 min). There is a 10% under-estimation and a 24% over-estimation for the analytical and simulated results. Although the error may seem large, it is worth noting that we are approximating complicated exit-missing costs using analytical and simulated models laden with simplifications and assumptions. Notably, the analytical model

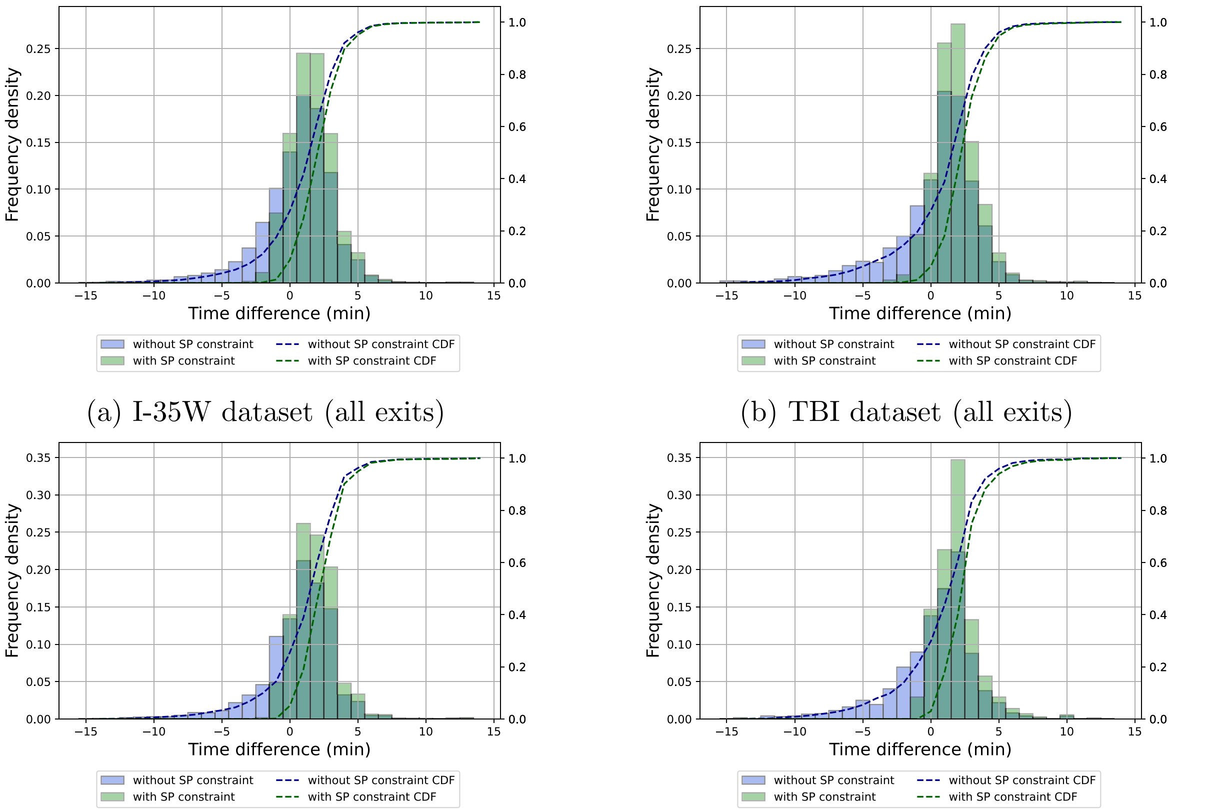

(a) I-35W dataset (all exits)
(b) TBI dataset (all exits)
(c) I-35W dataset (final exits)
(d) TBI dataset (final exits)

Fig. 6. Distributions of the time cost of missing exits and corresponding CDFs. Cost is calculated by subtracting the travel time of the alternative route from the travel time of the original route. Blue plots correspond to samples without the SP constraint in place. Green plots correspond to samples with the 10% SP constraint. (For interpretation of the references to colour in this figure legend, the reader is referred to the web version of this article.)

employs only five network variables to estimate these costs. Most importantly, the observations from all three approaches show that people tend to spend more time after missing an exit, yet the time costs are, on average, relatively low (approximately 2 min for Twin Cities). Therefore, lane changes intended to exit a freeway may not be strictly required if no opportunity for a safe lane change prior to the exit emerges. Drivers are thus resilient to missing exits.

The extra travel distance incurred by missing an exit is further evaluated. Fig. 7 presents the travel distance costs of missing exits for the two datasets, while the statistics of the distributions are summarised in Table 5. We hypothesise that by missing an exit, one would be penalised with extra travel distance. Thus, for our null hypothesis, we assume that the mean of the additional travel distance from missing exits is less than or equal to 0. The alternative hypothesis states otherwise. Once again, the p-values favour the alternative, and we conclude that a driver would be subjected to extra travel distance when missing an exit.

Likewise, we evaluate the discrepancies between empirical results and those derived from analytical and simulation methods for the distance cost. By combining the two datasets, the mean and standard deviation are 3.068 km and 2.272 km, respectively. Recall that the mean distance costs from the analytical and simulated means are 2.634 km and 3.145 km, while the standard deviations are 2.020 km and 3.409 km. The combined empirical means are therefore, 14% under-estimated by the analytical value and 3% over-estimated by the simulated value. The standard deviations, on the other hand, are 11% under-estimated and 50% over-estimated by the analytical and simulated methods. From the above analysis, it is clear that while the estimated means serve as reasonable approximations, the standard deviations diverge notably. In particular, the simulated standard deviation tends to surpass the empirical value by a margin. The large difference may be a result of the higher variability in the sampled data. Since the LEHD data cover large amounts of commuting ODs from each metro area, the variability between routes may be substantially different. This will in turn magnify the variance of the exit-missing costs. Nevertheless, the observations underscores that the exit-missing costs are not substantial.

4.2.2. Analysis on relative proportions

In general, evaluating whether an increase in travel time/distance is relevant for the drivers would require a discussion on what proportion of the total trip this represents. Therefore, we further evaluate the exit missing costs in terms of the relative proportions of the costs to their original trips.

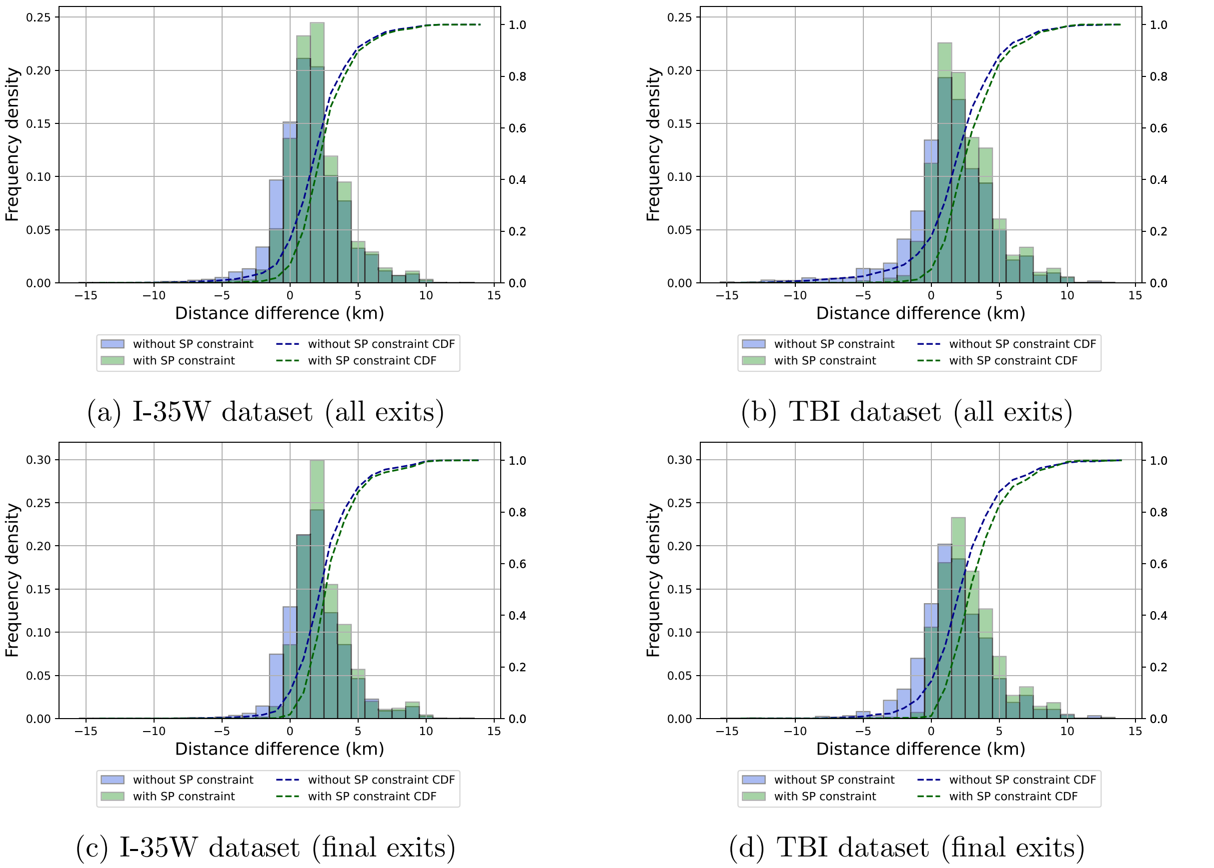

(a) I-35W dataset (all exits)

(b) TBI dataset (all exits)

(c) I-35W dataset (final exits)

(d) TBI dataset (final exits)

Fig. 7. Distributions of the distance cost of missing exits and corresponding CDFs. Cost is calculated by subtracting the distance of the alternative route from the distance of the original route. Blue plots correspond to samples without the SP constraint in place. Green plots correspond to samples with the 10% SP constraint. (For interpretation of the references to colour in this figure legend, the reader is referred to the web version of this article.)

Table 5
Summary of the distance cost of missing exits. (** $p \leq 0.01$, * $p \leq 0.05$).

		I-35W		TBI	
		Without SP constraint	With SP constraint	Without SP constraint	With SP constraint
All exits	Mean (km)	1.958	2.536	1.879	2.978
	Median (km)	1.900	2.218	1.967	2.582
	Std (km)	2.636	2.278	3.811	3.493
	Min (km)	−20.270	−16.548	−43.587	−4.677
	Max (km)	23.802	23.802	23.326	23.326
	Sample size	21,769	15,727	2,403	1,625
	p-value	0.000e−30**	0.000e−30**	0.000e−30**	0.000e−30**
Final exits	Mean (km)	2.452	3.041	2.382	3.370
	Median (km)	2.199	2.522	2.132	2.863
	Std (km)	2.479	2.235	2.949	2.630
	Min (km)	−36.717	−2.872	−12.249	−4.504
	Max (km)	23.697	23.697	23.164	23.164
	Sample size	12,329	7,936	1,240	715
	p-value	0.000e−30**	0.000e−30**	0.000e−30**	0.000e−30**

Fig. 8 illustrates the time costs as a percentage of the original trip length, while Table 6 summarises the statistics. Continuing from the t-tests performed for the absolute costs, in this section, we examine whether the mean percentage costs are also positive. The null hypothesis is set such that the mean values are assumed to be 0. The *p*-values for all scenarios are significant, indicating that, on average, the percentage time costs are not 0. In particular, for all our scenarios, the costs are positive. When the SP constraint is in place, the percentage time costs are approximately 12% for all exits and 14% for the final exits. Unsurprisingly, without the SP constraint, a portion of the distributions shifts to the negative range, and the mean proportional time costs drop.

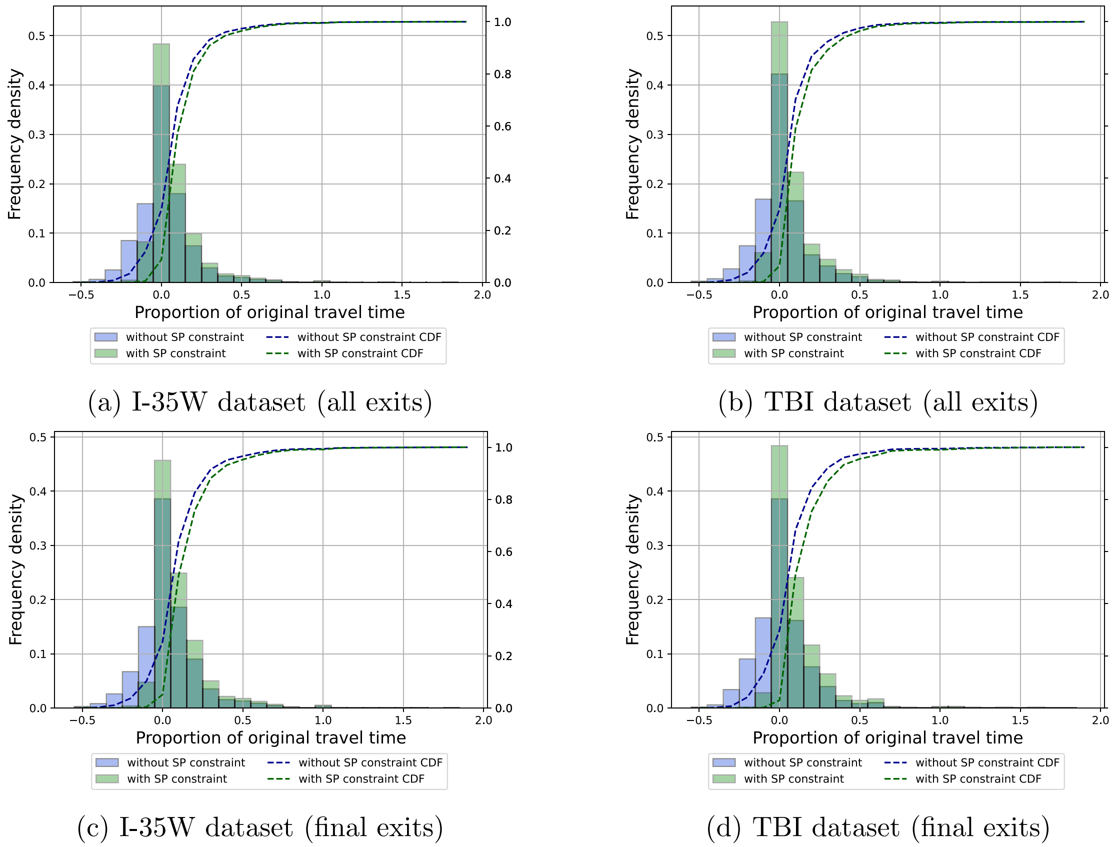

(a) I-35W dataset (all exits)
(b) TBI dataset (all exits)
(c) I-35W dataset (final exits)
(d) TBI dataset (final exits)

Fig. 8. Distributions of the time cost of missing exits and corresponding CDFs. Costs are in proportion of the original trip length.

Table 6
Summary of the time cost of missing exits in terms of the proportion of the total trip. (**$p \leq 0.01$, *$p \leq 0.05$).

		I-35W		TBI	
		Without SP constraint	With SP constraint	Without SP constraint	With SP constraint
All exits	Mean	0.0637	0.1194	0.0523	0.1201
	Median	0.0465	0.0769	0.0444	0.0769
	Std	0.2058	0.2013	0.2079	0.1594
	Min	−1.7143	−0.8182	−2.7857	−0.1667
	Max	4.6667	4.6667	1.8000	1.8000
	Sample size	21,769	15,727	2,403	1,625
	p-value	0.000e−30**	0.000e−30**	0.000e−30**	0.000e−30**
Final exits	Mean	0.0782	0.1476	0.0592	0.1427
	Median	0.0526	0.0952	0.0400	0.0952
	Std	0.2377	0.2417	0.1836	0.1776
	Min	−1.0000	−0.2500	−0.5385	−0.1250
	Max	4.3333	4.3333	1.6000	1.6000
	Sample size	12,329	7,936	1,240	715
	p-value	0.000e−30**	0.000e−30**	0.000e−30**	0.000e−30**

As for the percentage distance costs, the distributions are illustrated in Fig. 9, and the statistics are presented in Table 7. Again, the null hypothesis is set such that the mean values are 0. All p-values suggest that the distance percentage costs relative to the original trips are positive. The magnitudes of the costs with SP constraints are approximately 17% for all exits and 23% for final exits. The results above suggest that the percentage distance costs are typically larger than the percentage time costs. We speculate

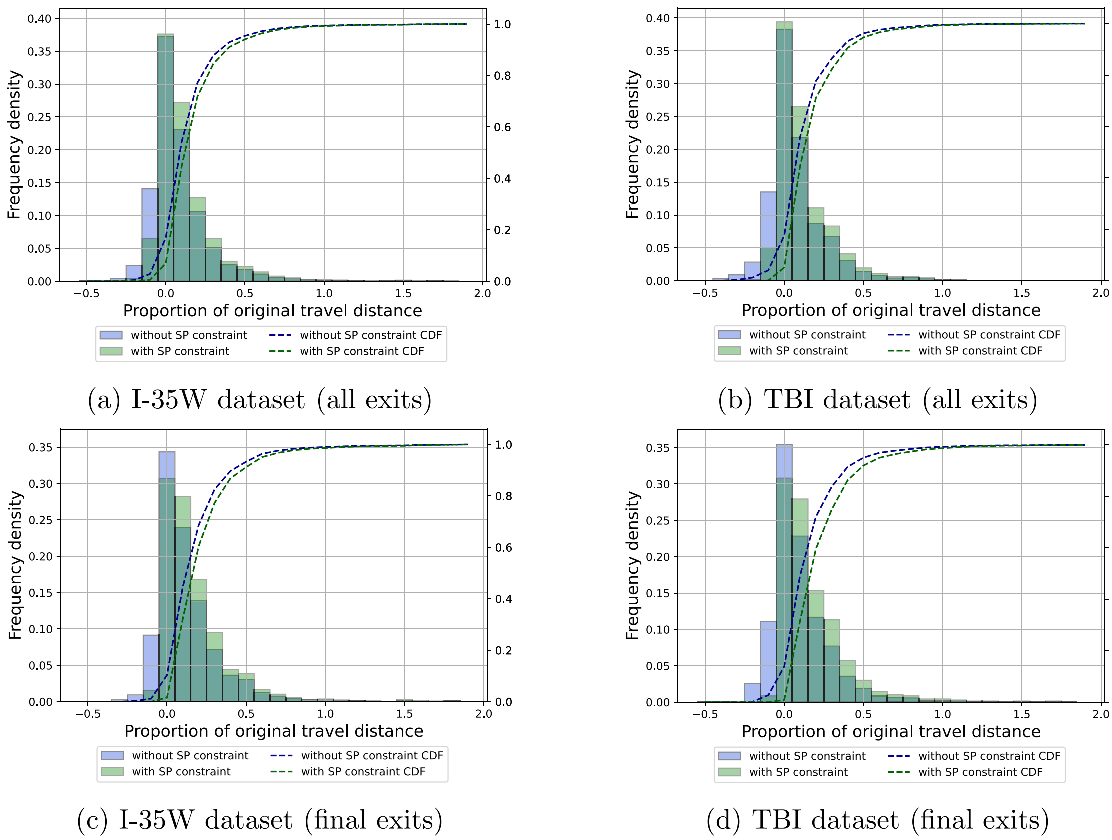

Fig. 9. Distributions of the distance cost of missing exits and corresponding CDFs. Costs are in proportion of the original trip length.

Table 7
Summary of the distance cost of missing exits in terms of the proportion of the total trip. (** $p \leq 0.01$, * $p \leq 0.05$).

		I-35W		TBI	
		Without SP constraint	With SP constraint	Without SP constraint	With SP constraint
All exits	Mean	0.1372	0.1743	0.1231	0.1736
	Median	0.0898	0.1130	0.0839	0.1166
	Std	0.2270	0.2379	0.2039	0.1939
	Min	−0.7571	−0.7571	−1.8837	−0.1250
	Max	4.4029	4.4029	2.0158	2.0158
	Sample size	21,769	15,727	2,403	1,625
	p-value	0.000e−30**	0.000e−30**	0.000e−30**	0.000e−30**
Final exits	Mean	0.1825	0.2313	0.1540	0.2243
	Median	0.1163	0.2313	0.1022	0.1740
	Std	0.2613	0.2842	0.2052	0.2243
	Min	−0.3694	−0.0497	−0.3184	−0.0719
	Max	4.3433	4.3433	2.0009	2.0009
	Sample size	12,329	7,936	1,240	715
	p-value	0.000e−30**	0.000e−30**	0.000e−30**	0.000e−30**

that this observation might be due to vehicles having to travel further down the freeway after missing an exit. The freeway section, which has much higher traffic speeds than local streets, then understates the marginal impact on travel time.

Furthermore, both the figures and tables show that the percentage costs are fairly consistent for the two datasets, suggesting a strong dependence of the exit-missing costs to the network in which the trips belong to. From both absolute and percentage costs, it can be seen that the cost tend to be higher for final exits than all exits. The fact that interim exits have higher flexibility for future route choice might have caused this phenomenon. The earlier an exit is missed, we believe the easier it is for the driver to adjust its route to make up for the costs.

Table 8
Summary table for the time cost of missing exits for commuting and non-commuting trips. ($^{**}p \le 0.01$, $^{*}p \le 0.05$).

		I-35W		TBI	
		All exits	Final exits	All exits	Final exits
Commuting	Mean (min)	1.599	1.957	2.016	2.167
	Median (min)	1	2	2	2
	Std (min)	1.759	1.819	1.785	1.523
	Sample size	3,510	1,688	189	168
Non-commuting	Mean (min)	1.616	1.768	1.808	1.857
	Median (min)	2	2	2	2
	Std (min)	1.688	1.575	1.669	1.653
	Sample size	12,217	6,248	1,436	1,262
p-value		0.595	2.548e−5**	0.111	0.022*

Table 9
Summary table for the distance cost of missing exits for commuting and non-commuting trips. ($^{**}p \le 0.01$, $^{*}p \le 0.05$).

		I-35W		TBI	
		All exits	Final exits	All exits	Final exits
Commuting	Mean (km)	2.472	3.224	3.221	3.763
	Median (km)	2.170	2.436	2.314	3.122
	Std (km)	2.448	2.655	2.743	2.464
	Sample size	3,510	1,688	189	168
Non-commuting	Mean (km)	2.554	2.991	2.947	3.318
	Median (km)	2.231	2.558	2.608	2.760
	Std (km)	2.227	2.105	2.458	2.646
	Sample size	12,217	6,248	1,436	1,262
p-value		0.059	1.444e−4**	0.155	0.039*

It can also be seen that the distributions with the SP constraint have a larger portion in the negative plane. However, instead of skewing to the left, the plot now skews to the right, indicating that trips with negative costs typically have high travel time or distance that forces the percentage costs low. Due to the invalidity of comparing excess routing original trips and shortest path alternatives, analysis hereafter are performed with the SP constraint in place.

4.2.3. Analysis on commuting effect

Unlike the data obtained from the LEHD dataset, GPS data used in this study consists of both commuting and non-commuting trips, providing an opportunity to examine the impact of trip purposes on exit-missing costs. Here, we only assess the "SP-constrained" scenario. The two-sample independent t-test is applied, assuming equal variances. The null hypothesis states that the expected values for the costs of missing exits for commuting and non-commuting trips are the same. The alternative states otherwise.

As above, both time and distance costs are examined. Figs. 10 and 11 demonstrate the cost distributions for commuting and non-commuting trips, and their statistics are summarised in Tables 8 and 9. Interestingly, all *p*-values for the final exit cases are significant, and in general, the average costs for commuting trips are larger than the average for non-commuting trips. This opposes our initial hypothesis and suggests that the costs of missing an exit are somehow related to the purpose of the trip. The cases involving all exits are not statistically significant due to the greater flexibility after missing an interim exit. In other words, when drivers miss an interim exit, they have more alternative routes available to them than if they missed the final exit. This flexibility allows drivers to more easily counteract the negative effects of missing an exit, which could downplay the impact of different OD locations, leading to seemingly consistent comparison outcomes.

An inspection of the trips containing final exits shows that the average distances between the final exit and the destination for commuting trips (2.992 km) and non-commuting trips (2.970 km) are barely different. Therefore, the flexibility of route choice is similar, and the discrepancy is likely related to the length of rerouting. The deviation factors are computed for both the original paths and the shortest paths (from the exit to the destination). Commuting trips are seen to have a higher average deviation (2.787 km) than non-commuting trips (1.720 km). The difference in the costs thus could not have been caused by a higher sensitivity of the commuting trips towards missing exits due to them travelling more frequently on the shortest path. Therefore, the cost discrepancy is likely related to the network configuration.

4.2.4. Analysis on peak hour effect

Considering that traffic congestion may play a crucial role in the composition of exit-missing costs, we examine the effects of travelling during peak hours. Again, we focus solely on the "SP-constrained" scenario. The analysis done in this section divides the trips into peak hour and off-peak hour ones based on the time that a trip was performed. A trip is deemed to have experienced peak hour effects if its entire duration falls within one of the following peak periods: morning peak (7–9 am) or afternoon peak (4–6 pm). These peak hours are considered only on weekdays.

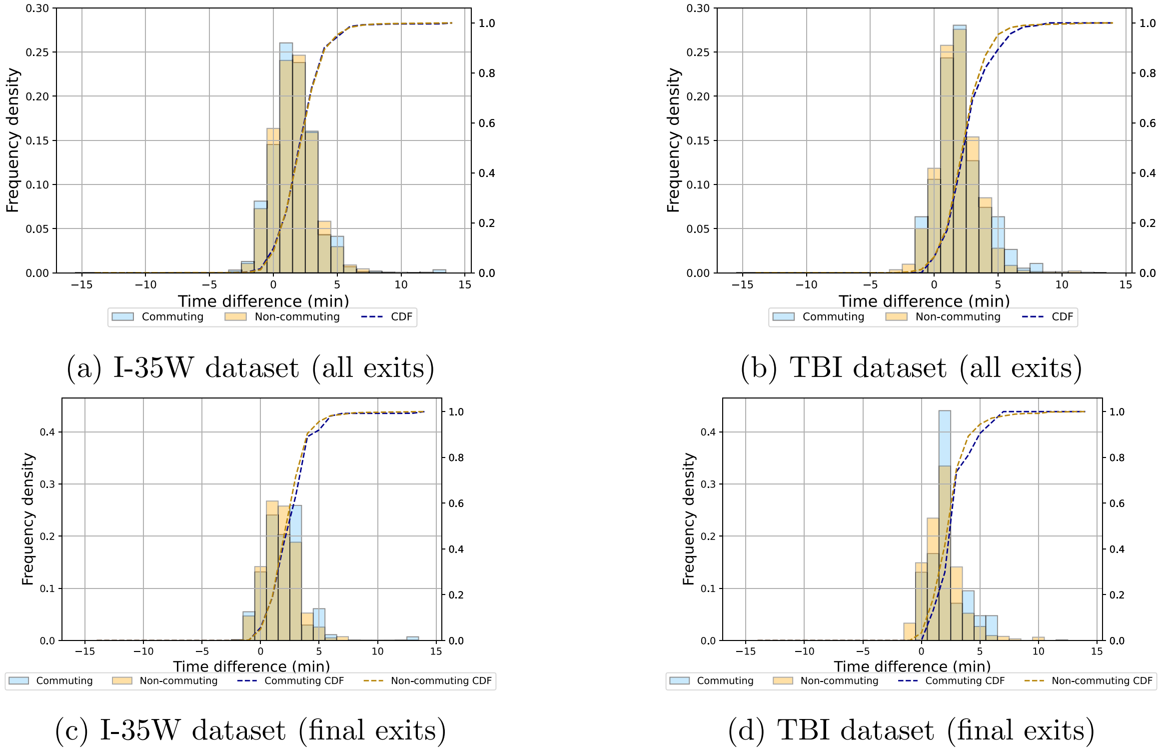

Fig. 10. Distributions for the time cost of missing exits in commuting and non-commuting trips and the corresponding CDFs.

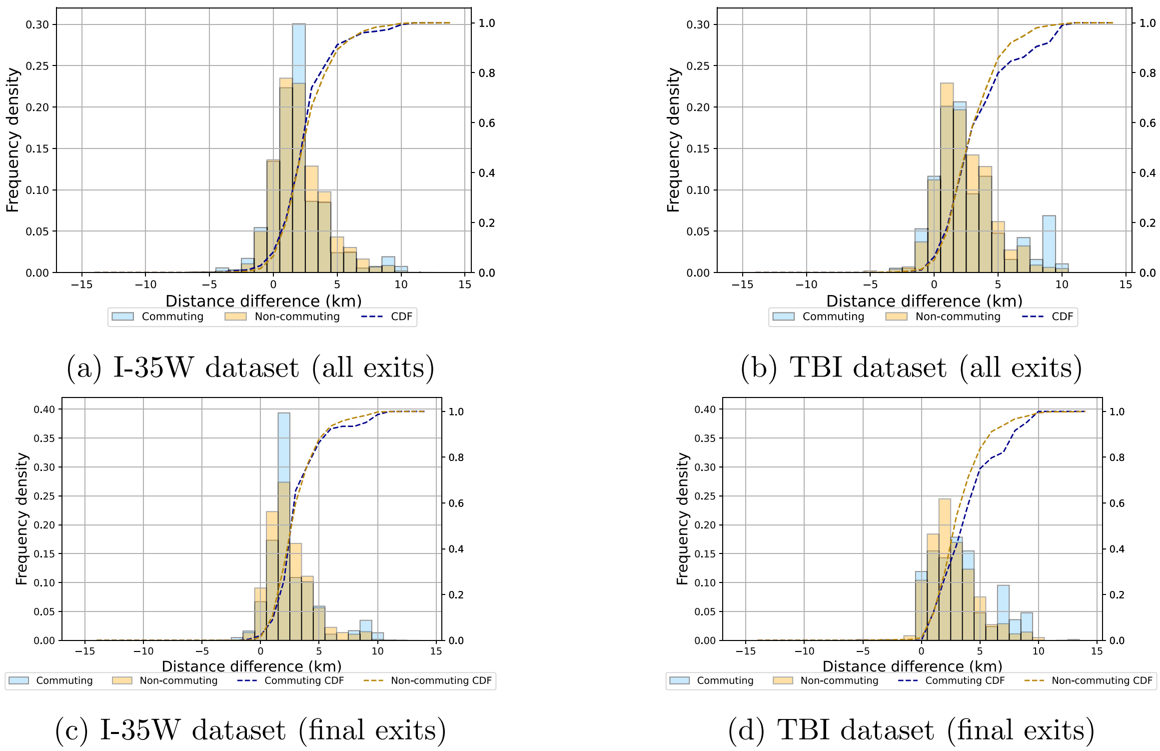

Fig. 11. Distributions for the distance cost of missing exits in commuting and non-commuting trips and the corresponding CDFs.

Table 10
Summary table for the time cost of missing exits for peak hour and off-peak hour trips. (**$p \le 0.01$, *$p \le 0.05$).

		I-35W		TBI	
		All exits	Final exits	All exits	Final exits
Peak hour	Mean (min)	1.677	1.944	2.084	2.1468
	Median (min)	2	2	2	2
	Std (min)	1.756	1.721	1.923	1.7786
	Sample size	4,538	2,374	238	109
Off-peak hour	Mean (min)	1.586	1.751	1.789	1.8482
	Median (min)	1	2	2	2
	Std (min)	1.682	1.588	1.636	1.6130
	Sample size	8,486	5,562	1,387	606
p-value		2.536e−3**	1.421e−6**	0.013*	0.080

Table 11
Summary table for the distance cost of missing exits for peak hour and off-peak hour trips. (**$p \le 0.01$, *$p \le 0.05$).

		I-35W		TBI	
		All exits	Final exits	All exits	Final exits
Peak hour	Mean (km)	2.512	3.057	2.864	3.226
	Median (km)	2.190	2.553	2.767	2.906
	Std (km)	2.311	2.247	2.165	2.085
	Sample size	4,538	2,374	170	109
Off-peak hour	Mean (km)	2.545	3.034	2.992	3.396
	Median (km)	2.220	2.522	2.539	2.845
	Std (km)	2.265	2.230	2.529	2.717
	Sample size	11,189	5,562	1,455	606
p-value		0.411	0.674	0.527	0.534

Figs. 12 and 13 illustrate the time and distance cost distributions, taking into account the effects of peak hours. Tables 10 and 11 present the statistics corresponding to the two figures. The t-tests were conducted with the null hypothesis that the costs during peak and off-peak hours are equivalent. Notably, none of the distance costs exhibit a significant p-value, indicating that the distance costs from missing exits during peak and off-peak periods tend not to differ. On the other hand, a majority of the time costs are shown to be statistically significant. Given the consistency in distance costs, the variation in time costs might be explained by the deteriorating traffic condition during the peak hours. This is further corroborated by the higher average costs observed during peak hour instances. Although the p-value is not significant for the final exits of the TBI dataset, the peak hour mean remains considerably higher than the off-peak mean. The insignificant p-value might be attributed to a smaller sample size compared to other cases.

From the figures, particularly the CDFs, it is evident that the time cost distributions for peak hour trips are generally more platykurtic. This trend arises because alternative routes that are longer than the original ones, leading to positive exit-missing costs, experience increased time costs due to slower traffic. Similarly, original routes that are longer than their alternative counterparts, resulting in negative costs, also have their travel time amplified, which further decreases the time cost (resulting in more negative values). This rationale underscores our decision to focus solely on the SP-constrained cases. The unconstrained distributions, with a significant portion below 0, would yield more negative costs during peak hours, potentially skewing the results. The SP cases are thus more compelling given that the two routes are more comparable. Thus, the empirical results identify the presence of traffic congestion during peak hours. The lowered speed during peak hours tends to magnify the time cost of missing exits, whereas the distance costs remain relatively unchanged.

5. Conclusions and limitations

This study ascertains the costs of missing exits, thereby exploring the benefits of performing lane changes for exiting freeways. First, an analytical model is proposed, whereby the exit-missing costs are deconstructed into sub-components with their values then estimated. Both the mean and standard deviation of the costs can be approximated. The proposed analytical methodology is then applied to the top 50 metropolitan regions in US. and the outcomes are compared with simulated values. The results demonstrate that the proposed analytical approach is practicable and can provide valuable insights into the nature of costs associated with missed exits. Specifically, networks with lower circuity, faster freeway speeds, and faster local street speeds often have higher costs associated with missing exits. Furthermore, if a network has sparser exit density and greater distances between exits, the costs for missing an exit tend to be high. However, inhomogeneous exit distributions can cause the prediction to overshoot the actual costs by a margin. Therefore, the model would perform satisfactorily in areas where exits are more homogeneous, such as in urbanised areas. Subsequently, we conduct a thorough analysis of two real-life empirical datasets obtained from the Minneapolis - St. Paul region. The results from both datasets are similar and also correspond with the analytical and simulated outcomes. All three analyses indicate that although missing exits can lead to higher travel costs, the increase is negligible, amounting to only a few minutes or kilometres.

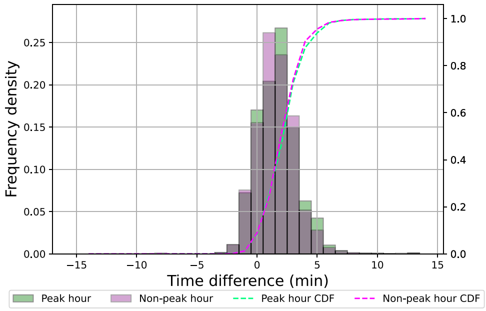

(a) I-35W dataset (all exits)

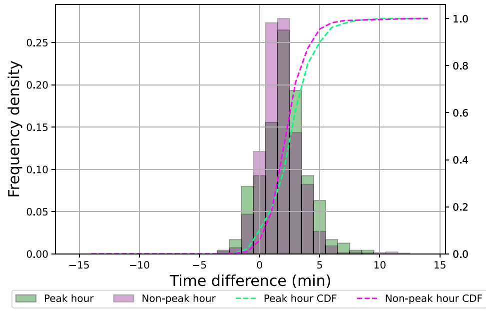

(b) TBI dataset (all exits)

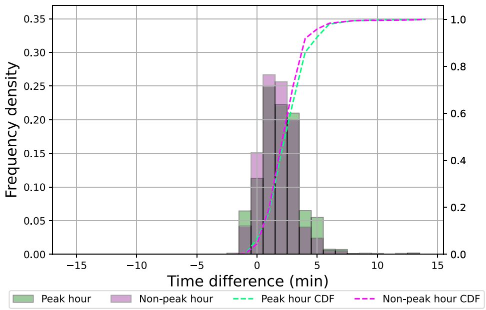

(c) I-35W dataset (final exits)

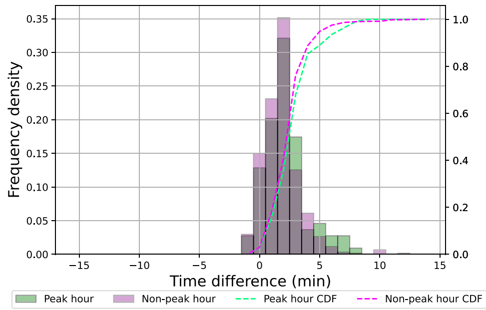

(d) TBI dataset (final exits)

Fig. 12. Distributions for the time cost of missing exits in peak hour and off-peak hour trips and the corresponding CDFs.

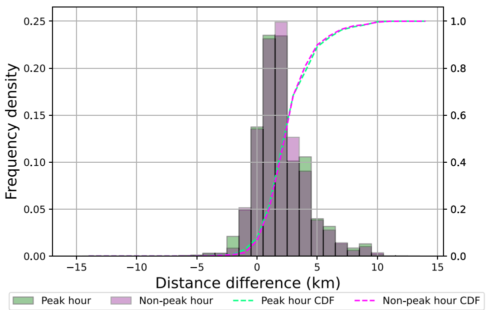

(a) I-35W dataset (all exits)

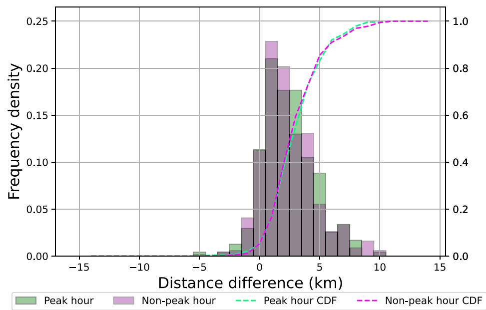

(b) TBI dataset (all exits)

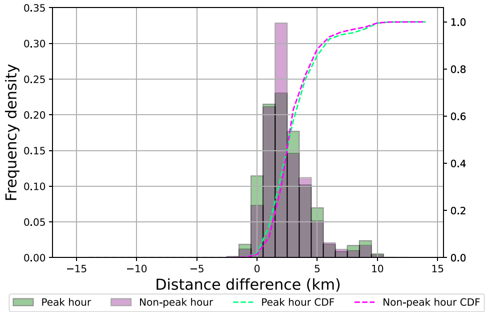

(c) I-35W dataset (final exits)

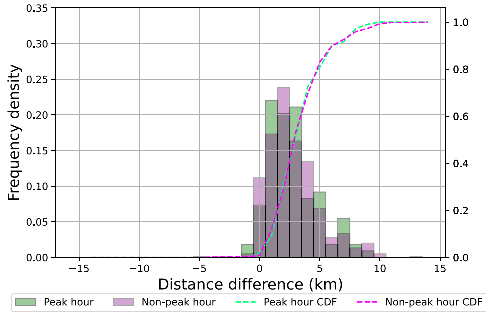

(d) TBI dataset (final exits)

Fig. 13. Distributions for the distance cost of missing exits in peak hour and off-peak hour trips and the corresponding CDFs.

These findings shed light on the costs associated with not executing a lane change to exit off-ramps. When lane changes are performed to avoid obstacles, the costs are essentially infinite, given that the maneuver prevents the driver from being indefinitely stuck. In contrast, the costs tied to not changing lanes for exiting freeways are notably lower. This discrepancy might partially explain why drivers occasionally miss their intended turns. As such, we recommend more lane change models to incorporate the probability of drivers missing exits, which could arise from factors such as fatigue, distractions, or underestimations of the complexity of a lane change maneuver. For the design of lane change controllers, our study can assist in balancing the trade-off between executing a lane change and enduring a longer route to the destination.

Given the distinct benefits of making a lane change to exit a freeway versus doing so to avoid blockage, we categorise the mandatoriness of lane changes into three levels: discretionary, expedient (ELC), and mandatory. The respective benefits of these lane changes are on the scale of seconds/metres, minutes/kilometres, and infinite. Based on our findings, we classify lane changes for tactical routing as ELC. Future studies should assess the benefits of other types of MLCs, such as obeying lane usage indications or yielding to emergency vehicles, to determine if they should also be classified as ELCs.

The present study is subject to several limitations, and we will first discuss the ones for the analytical model:

- As part of the cost functions, the contribution of exits to the surrounding households (in Section 2.1) is formulated based on the assumption that people are rational and fully aware of the travel time to their destinations. In fact, it has been previously demonstrated that drivers are not always rational and often do not travel on the shortest available path (Zhu and Levinson, 2015; Dia, 2002; Jiang et al., 2020). Therefore, the deterministic proportions we derived may not accurately reflect the true contribution of nearby exits. Since the experiment we conducted in Section 3 is based on the shortest path assumption, the potential ramifications of this limitation may not be readily apparent. However, future research should address this shortcoming by incorporating route choice techniques into the model.
- It is postulated in the proposed model that exits are characterised by a homogeneous Poisson point process, which represents a simplified approximation of the true distribution. In practice, the design of exit locations would be more dependent on the population of the surrounding neighbourhood, the spatial distribution of freeways, and the overall accessibility of the region. However, accounting for all possible scenarios would make our model overly complex and would require the computation of input parameters such as the locations of city centres and the density of links on the freeway network.
- As demonstrated in Section 3, the predicted value exhibits a strong dependence on the number of off-ramps from the street network. In our examples, the high variation in exit density and exit gap length led to the predictions to overshoot the actual values in regions with a larger area and fewer off-ramps. This is essentially a repercussion of the underlying HPPP assumption, which makes the model sensitive to fluctuations in the number of exits in subsets of the regions. Therefore, instead of computing the costs for a large geographical area, our model would perform better for areas where the density of exits is more consistent (e.g. urbanised area instead of the entire metropolitan area).
  It should be noted that the findings we have obtained are based on the average costs for an overall network. In dense urban area, with a lot of redundancy, missing an exit would not cost much if there is no congestion. However, in a sparser network, that may not be the case. Examples such as SLC and LAS have sparse networks and are observed to have relatively high costs associated with missing an exit.
- Finally, our analytical model fails to take into account supply side influences. As an example, higher flows are observed closer to the city centre than in rural areas. Thus higher weights should be placed on exits in more populated areas where the traffic network is denser and shorter exit-missing costs are expected.
  In addition, both the analytical and simulated models have omitted the impact of traffic congestion on the costs. As highlighted in Section 4.2.4, heavier traffic is observed to impact exit-missing costs, particularly the time cost. This suggests that further research should be undertaken to incorporate congestion into the cost modelling. However, in the absence of link-wise speed data for different time periods, we will defer this inquiry to future research. Likewise, the fluctuations in traffic flow can influence exit choice of drivers, which could, in turn, impact the exit-missing costs. In particular, a driver may opt for an earlier exit due to a downstream blockage or choose a later exit due to spillback from the usual off-ramp. In summary, factors such as spillbacks from bottlenecks can greatly affect route choices and consequently, lane-changing decisions and costs. It is challenging to disentangle the effects of congestion from path choice. The impact may be more visible if newer datasets are used, which reflect a wide spread of communication and technology systems where drivers may follow directions from navigation apps. The impact of such path planning behaviour on the costs of missing exits may be explored in future research by comparing old and new travel patterns.

The following are the limitations of our empirical analysis:

- The empirical datasets only cover the Twin Cities region. As a result, it remains unclear whether the same findings can be extrapolated to other regions. It is important to note that the performance of traffic networks is heavily influenced by their structural characteristics (Xie and Levinson, 2007). Therefore, high variability of travel costs may exist for networks with different configurations and road densities.
- The estimation of trips with missed final exits is based solely on a set of simple rules, without knowledge of the actual intentions of drivers. This approach may not accurately capture the complexities of real-world driving behaviours. A more accurate analysis could be achieved through the use of a driving simulation or an in-vehicle dataset that provides detailed vehicle indicator information and tracks driver intent.

- The alternative routes computed are assumed to follow the next downstream exit, which may not be a valid assumption. After missing exits, drivers will likely follow their intuitions to navigate to the destinations, which may not involve the exit directly downstream of the missed one. To address this issue, future research could incorporate data capturing drivers' actual behaviours after missing exits, which would provide a more accurate representation of travel patterns.
- The presence of in-car navigation may also influence the human reaction after an exit is missed. This factor was not directly accounted for in our analysis, since it is unknown which individuals used in-car navigation during the data collection period. However, we have indirectly considered this by purposefully selecting two datasets that were not collected recently (2008/09 and 2010/11, respectively). At that time, in-car navigation systems were not widely available, and only a fraction of people in the US used such systems regularly (Leshed et al., 2008). Moreover, Google Maps was released in September 2008, so its influence on the route choice decisions of drivers in the I35-W dataset should be minimal. Regarding the TBI dataset, there might have been a broader adoption of in-car navigation systems by 2010 than in 2008. Nonetheless, based on the shortest path usage analysis in Appendix D, we believe the impact of GPS navigation on exit choices would not significantly influence the calculated costs. After in-car navigation become wider adopted (in more recent years), we anticipate that there might be changes to the costs of missing exits as people are more likely to travel on the shortest paths, and concern about unfamiliarity routes might diminish.
- By utilising trajectory data from GPS records, we may have overlooked the influence of human factors on the exit-missing costs, such as variations in the Value of Time (VOT) and drivers' perceived travel costs. VOT differs among individuals and for different trip purposes, making exit-missing costs situation- and individual-dependent. For instance, the costs associated with missing an exit during a leisure trip would differ from those during a trip to a time-sensitive meeting. However, this study focuses solely on objective costs incurred when exits are missed, omitting demand-side factors. To assess the impact of VOT on the cost of missing freeway exits, future studies should investigate the marginal disutility of travel costs for various types of trips and for different driver populations. For research related to commuting VOT, interested readers can refer to Li et al. (2010), Carrion and Levinson (2012).

  Furthermore, the costs perceived by human drivers may differ from the actual costs incurred on the road. Perceived costs can depend on various factors, including the driver's familiarity with the road, the nature of the trip, the driver's expected arrival time, and individual variations. As an example, individuals may encounter discomfort while navigating an unfamiliar route. Missing a frequently used exit and travelling into an unfamiliar area can significantly impact the urgency of a lane change. In such cases, the lane change may feel "more mandatory" than the objective costs incurred. Extracting this information can be challenging and may require an understanding of the mismatch between drivers' expected and actual utilities. Future research should explore how mandatory a lane change feels to a driver using datasets beyond trajectory data. Surveys can gauge drivers' attitudes towards distracted driving and VOT, while driving simulator experiments, or in-vehicle monitoring, coupled with electroencephalogram technologies, may be better suited for investigating the cognitive processes and emotional responses while driving, offering insights into unconscious processes.

As for future research directions, our findings can be applied to model lane changes when dealing with the trade-off between safety and travel time/fuel consumption (Ji and Levinson, 2021; Ji et al., 2023a,b). The analytical model we proposed can be integrated into the cost functions by allowing a certain degree of stochasticity in the merging process. Moreover, our work can provide insight into exiting activities for traffic simulations. Existing microscopic models use rules to model lane changes in preparation for exits. For instance, VISSIM adopts two criteria for exiting: the lane change distance and the emergency stop distance. The lane change distance specifies the distance from which the driver becomes aware of the upcoming exit and will consider it in lane change maneuvers. The emergency stop distance is the distance from the exit the driver will stop to wait for an acceptable gap to change lanes. On the other hand, AIMSUN uses a look-ahead heuristic, which reduces the chance of a vehicle coming to a stop to exit. However, the same assumption is made that a car will force a gap in the target lane when executing the lane change, which often causes the traffic condition to deteriorate as vehicles build up (Barceló, 2010). We argue that such an assumption can be relaxed given that the cost of missing an exit is relatively small in most urban cases, and the vehicle will eventually route back to its destination when necessary.

The findings of this study challenge the conventional notion of MLC and suggest a need for researchers to refine existing lane change models.

CRediT authorship contribution statement

Zhaohan Wang: Writing – original draft, Software, Methodology, Investigation, Conceptualization. **Mohsen Ramezani:** Writing – review & editing, Supervision, Project administration, Methodology, Investigation, Funding acquisition, Conceptualization. **David Levinson:** Writing – review & editing, Supervision, Project administration, Methodology, Investigation, Funding acquisition, Conceptualization.

Acknowledgements

This research was partially funded by the Australian Research Council [grant number DP220100882].

Table 12
List of main notations.

Notations	Definition (*unit*)
	Network Variables
D	The distance cost of missing exits (km)
D_F	The distance cost of missing exits on freeway network (km)
D_S	The distance cost of missing exits on surface street network (km)
T	The time cost of missing exits (min)
C	The network circuity
d_f	The intermediate gap length between freeway exits (km)
v_f	The travel velocity on freeway network (km/min)
v_s	The travel velocity on surface street network (km/min)
	Point Process
$\mathbb{R}$	Set of real numbers
$\mathbb{1}$	The indicator function
$\mathbb{P}$	The probability of an event occurring
$\mathbb{E}$	The expectation of a random variable
μ	The population mean of a random variable
σ	The population standard deviation of a random variable
Φ	A point process in $\mathbb{R}^2$
B	A Borel set of the underlying point process Φ
ψ	The simple counting measure of B, defined as $\psi(B) = \sum_{x_i \in \Phi} \mathbb{1}(x_i \in B)$
Λ	The intensity measure of points in B defined as $\Lambda(B) = \mathbb{E}[\psi(B)]$
ℓ	The Lebesgue measure of subset B
λ	The intensity of the point process Φ
Γ	The gamma function defined as $\Gamma(z) = \int_o^\infty t^{z-1} e^{-t} \mathrm{d}t$
f/F	Probability/Cumulative distribution function of a random variable
R_n	The random variable representing the distance between a randomly chosen point and its nth nearest neighbour in the point process
r_n	The distance between a particular point and its nth nearest neighbour in a given point process. It can be thought of as a particular realisation of R_n
g	A multivariate function representing either the time or the distance cost function

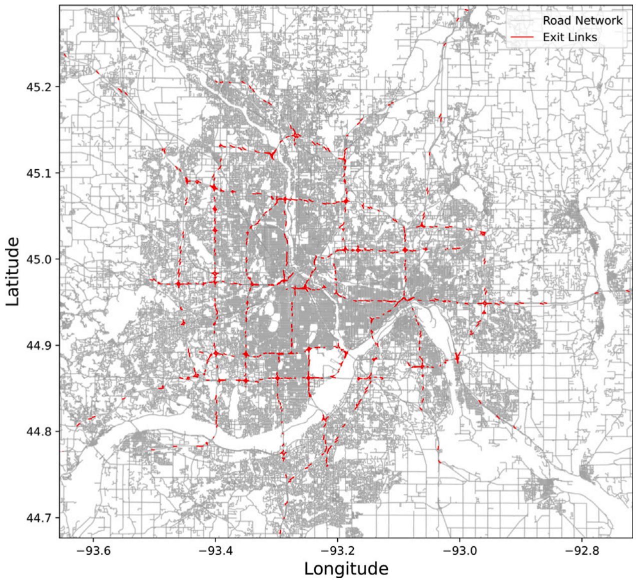

Fig. 14. Spatial location of all exits in the datasets.

Appendix A. Notation

See Table 12.

Appendix B. Exits analysed

See Fig. 14.

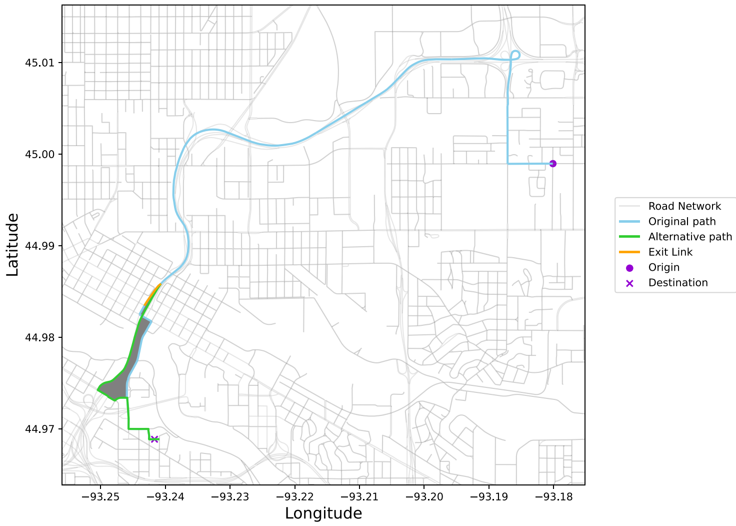

Fig. 15. Original and alternative routes of trip 497 from sample GPS1019. The deviation of this original-alternative pair is calculated as the square root of the shaded area.

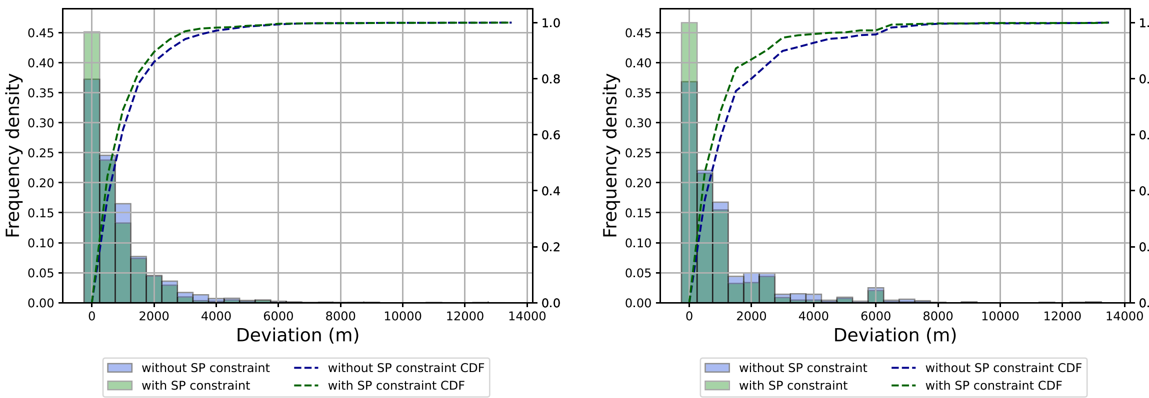

(a) I-35W dataset (b) TBI dataset

Fig. 16. Route deviation distributions and CDFs between original and alternative routes from final exits. Blue plots correspond to samples without the SP constraint in place. Green plots correspond to samples with the 10% SP constraint. Subplots (a) and (b) correspond to the I-35W dataset and the TBI dataset, respectively. (For interpretation of the references to colour in this figure legend, the reader is referred to the web version of this article.)

Appendix C. Route deviation and circuity

In this appendix section, we compute the circuity for both original and alternative routes to ascertain whether there is a change in circuitousness by missing an exit. To quantify the discrepancy between the original and the alternative routes, we employ the route deviation, which measures the closeness between two trajectories with the same OD. The measure is computed from the square root of the area of the concave hull that is enclosed by the routes (Wang et al., 2022). A higher deviation suggests that the alternative path is more dissimilar to the original path and, by our assumption, may imply higher routing costs. Fig. 15 shows an arbitrary trip and its best alternative. In this case, the alternative readjusts itself back to the original route after exiting at the next downstream ramp. The deviation from missing the exit can be derived from the square root of the shaded area.

Fig. 16 shows the distributions of deviation for final exits. As shown in the figure, 90% of the exiting samples have deviations less than 3 km, reinforcing that alternative routes may not be very dissimilar to their original pair. Furthermore, it is expected and observed that original routes with the SP constraint deviate less from their alternatives since both paths have optimised travel times.

To understand the impact of missing an exit on the directness of the trips, we utilise the network circuity, which is computed as the ratio between the route length and the Euclidean distance between the origin and the destination. Circuity is computed for

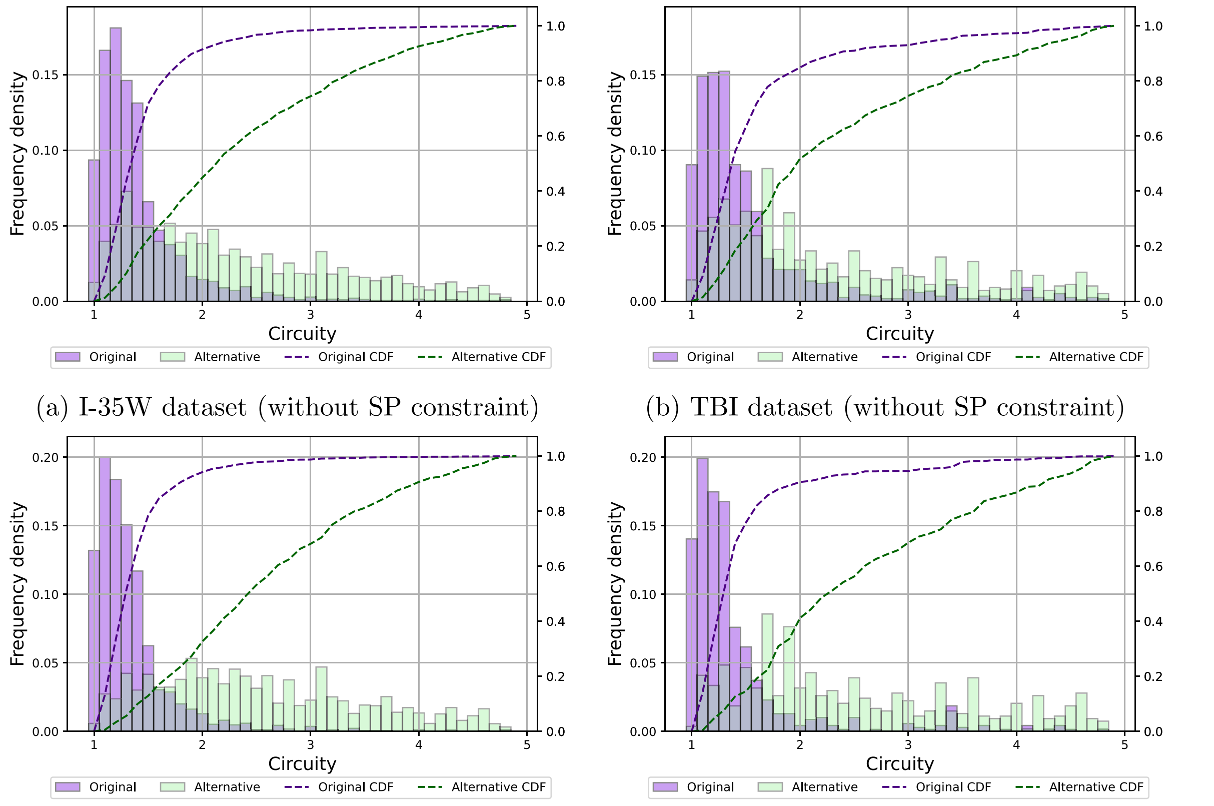

(a) I-35W dataset (without SP constraint)
(b) TBI dataset (without SP constraint)
(c) I-35W dataset (with SP constraint)
(d) TBI dataset (with SP constraint)

Fig. 17. Circuity distributions and CDFs for original and alternative routes from final exits. The purple plots correspond to the original routes, and the green plots correspond to the alternative routes. Subplots (a) and (c) correspond to the I-35W dataset and subplots (b) and (d) correspond to the TBI dataset. (For interpretation of the references to colour in this figure legend, the reader is referred to the web version of this article.)

original and alternative routes from the source node of the exit to the final destination of the trip. The outcomes are illustrated in Fig. 17. As can be seen, the densities of the original routes are more concentrated at lower values, while the alternative routes are more platykurtic. Although computed with shortest path assumptions, the alternative routes have a spread-out distribution due to the great variability of the Euclidean distance between the assessed ODs. In general, we assume a shorter distance between the exit source node and the destination will induce a larger circuity as there is a higher likeliness of taking detours, but this may also depend on the road network topology.

Moreover, we compare the deviation factors to the change in circuity and exit missing costs, evaluating our hypothesis that a larger deviation can induce larger time and distance discrepancies. The correlations are assumed to be linear, and the Pearson correlation coefficients are calculated between the variables. As shown in Table 13, only the costs are strongly correlated, while the deviation has weak correlations with other variables. This suggests the deviation is not suited for estimating the costs of missing an exit. Although counter-intuitive, considering the opposing effect of the negative time/distance costs may explain this outcome. In addition, the deviation is not only related to the closeness of the original and alternative trajectories but also their length. This adds a stochastic nature to the parameter. Therefore, although the deviation is a fair measure of the spatial variation of two routes, it can be misleading when used as a parallel comparison standard. On the other hand, the circuity difference is seen to have a moderate positive correlation with the costs, indicating that more circuitous routes correspond to higher travel costs. Unsurprisingly, the travel costs themselves have a strong positive correlation as the average velocities on alternative routes are guaranteed to be positive.

Appendix D. Categorical analysis of final exits

In this section, we demonstrate our method of estimating the number of final exits missed by the participants. Here we only assess the final freeway exits since the intention of remaining on the freeways for the interim exits is ambiguous as there is higher flexibility for a driver to choose an interim exit than it is for a final exit. We also neglect non-commuting trips since inconsistent OD pairs can generate distinctive routes with different choice sets of exits. For each driver, we split all commuting trips into to-home and to-work. The I-35W dataset (VMT and Otrec combined) is further stratified into before-bridge-reopen and after-bridge-reopen, ensuring bridge usage consistency.

Table 13
The correlation between measurements of missing exits. The factors are: the extra travel time cost, the extra travel distance cost, the circuity difference, and the routes deviation.

Factors	1	2	3	4
1. Travel time cost	–	0.736***	0.433**	−0.368*
2. Travel distance cost		–	0.523**	−0.207*
3. Circuity difference			–	−0.187*
4. Route deviation				–

***: Strong correlation ($0.7 < |r| < 1$).
**: Moderate correlation ($0.4 < |r| < 0.7$).
*: Weak correlation ($0.1 < |r| < 0.4$)

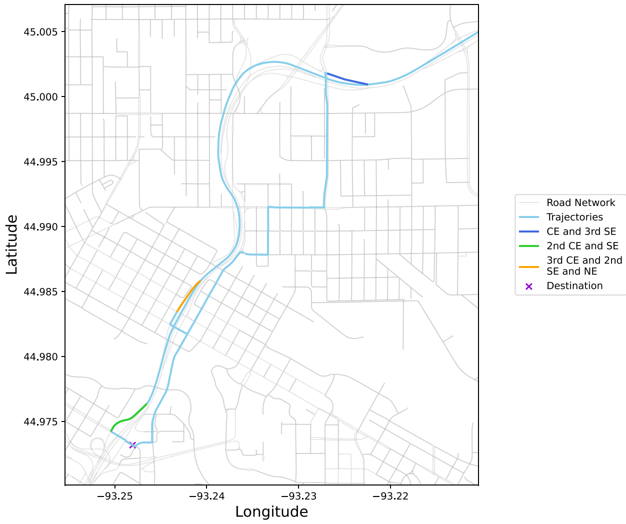

Fig. 18. Final exits of to-work trips for sample GPS2038. The subject used three different exits during the sampling period. Common Exit (CE) denotes the ordering of the final exits regarding the frequency of usage; Shortest Exit (SE) corresponds to the ordering of the exits based on their usage in the nth shortest paths (from the source node of CE to the destination marked by the purple cross); Next Exit (NE) is defined as the next exit directly downstream of the CE, which we assume a trip that missed the CE has traversed along.

The final exits under each subcategory are extracted and sorted according to their proportion of appearance, where the most frequent exit is assigned to be the Common Exit (CE). We then retain only the downstream exits of the CE by applying the breadth-first search algorithm on the freeway and ramp network for each distinctive commuting OD pair.

The remaining exits are ranked based on the order of shortest path using a variant of the path deletion K-shortest paths algorithm (Azevedo et al., 1993). The algorithm incrementally eliminates the final exit in the fastest route, which forces the algorithm to search for a new shortest path with a different final exit. The loop stops once the analysed exit is matched with the final exit of the shortest path. The order of the Shortest Exit (SE) is then recorded.

In addition, we identify the Next Exit (NE) downstream of the CE for each OD pair by running a single source Dijkstra search starting at the CE source node. NE can be obtained as the exit edge with the least cost assuming equal link impedances on all edges, excluding the CE. Trips in the same OD pair that contain the NE are then identified and classified as trips with missing exits if and only if their proportion of appearance in their respective OD pair is less than equal to certain threshold. Otherwise, it is assumed to be intentional. In this paper, we set the thresholds to be 25%, 15%, and 5%.

Above we have developed a simple heuristic to categorically analyse the exits based on their frequency of usage, travel time to destination, and likeliness of being missed. The three labels are illustrated in Fig. 18 through an arbitrary commuting OD pair. The CE, in this case, has the highest travel time out of the three options, which in turn emphasises that people are often not rational in their route choice. The implementation of the procedure is showcased in Algorithm 1.

Following the aforementioned procedure, 2,888 final exits from commuting trips are used to analyse the exiting behaviour of drivers. After assigning the labels to all final commuting exits, the counts are aggregated, and the output is presented in the format of a decision tree (Fig. 19). The branches of the trees represent the decisions regarding ordering, while the leaves represent the percentages of the corresponding orders.

Looking top-down from the decision tree, the large majority (roughly 98%) of the final exits are comprised of CEs, while at most, three exits were used by participants during the sampling period. This suggests people tend to minimise variation by sticking to a fixed commuting route.

Furthermore, we see that the CEs are often not the SEs (13.19% for the I-35W dataset and 18.90% for the TBI dataset) even from the point just upstream of the CE. Previous studies (Zhu and Levinson, 2015; Tang and Levinson, 2018) on the same datasets

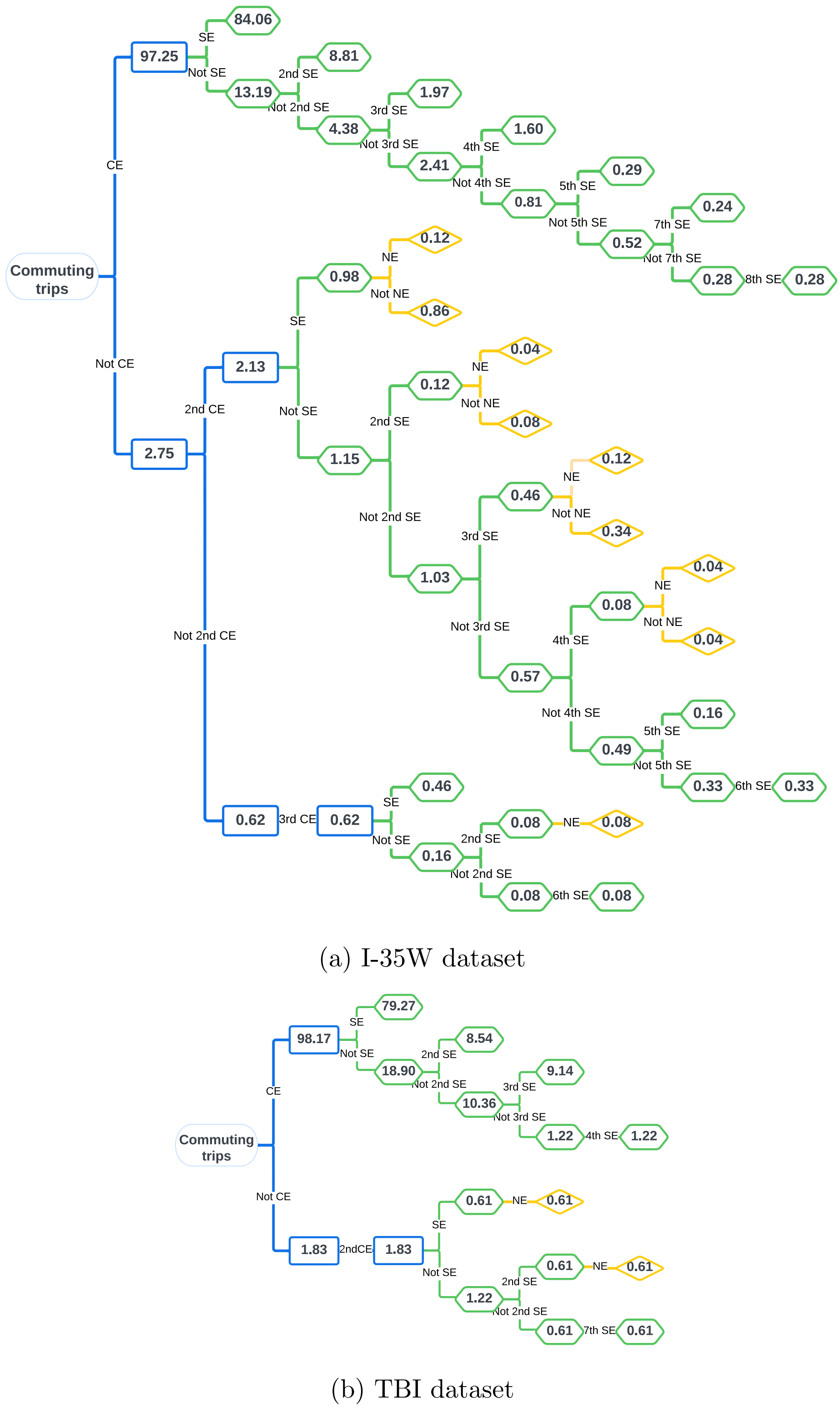

Fig. 19. Decision tree of exit structures for commuting trips. All numbers on leaves are in percentage. Blue corresponds to the order of CE; green corresponds to the order of SE; orange corresponds to the binary decision of NE. (For interpretation of the references to colour in this figure legend, the reader is referred to the web version of this article.)

Algorithm 1 Exit Class Identification

Input:

OD_{list}: A list of OD vectors with each vector containing different numbers of trips. Each trip (element of a vector) contains different links

Output:

$final\_exits[OD]$: For each OD, a table that contains the exits used in that OD pair along with the counts, CE, NE, and SE orders

Definitions:

(U_i, V_i): Source and target nodes of a link i
G: Road network graph
G_{freeway}: A subgraph of the road network graph containing freeway network only
BFS(graph, start, depth): Breadth-first search function
dijkstra(graph, start, end): Dijkstra's shortest path function

for each OD in OD_{list} **do**
    for each $trip$ in OD **do**
        Extract the final exit $(U_{\text{exit}}, V_{\text{exit}})$ from trip
        $final\_exits[OD] \leftarrow (U_{\text{exit}}, V_{\text{exit}})$
    end for
    $exit\_counts \leftarrow$ count occurrences of each unique$(U_{\text{exit}}, V_{\text{exit}})$ in $final\_exits$
    $CE\_exit \leftarrow$ argmax$(exit_counts)$
    $down\_links \leftarrow$ BFS$(graph = G_{\text{freeway}}, start = U_{CE_exit}, depth = 20)$
    $down\_exits \leftarrow final\_exits \cap down\_links$
    for $(U_{\text{exit}}, V_{\text{exit}})$ in $down\_exits$ **do**
        $CE[(U_{\text{exit}}, V_{\text{exit}})] \leftarrow$ ranking of $(U_{\text{exit}}, V_{\text{exit}})$ in $exit\_counts$
        $NE[(U_{\text{exit}}, V_{\text{exit}}) | (U_{\text{exit}}, V_{\text{exit}}) = down\_exits[2]] \leftarrow 1$
        set $k \leftarrow 1$
        while True **do**
            $SP \leftarrow$ dijkstra$(graph = G, start = U_{CE_exit}, end = V_{destination})$
            if $(U_{\text{exit}}, V_{\text{exit}}) \in SP$ **then**
                $SE[(U_{\text{exit}}, V_{\text{exit}})] \leftarrow k$
                break
            else
                $G \leftarrow G - \{\text{last exit in } SP\}$
            end if
            $k \leftarrow k + 1$
        end while
    end for
    $final\_exits[OD] \leftarrow$ sort $final\_exits[OD]$ based on unique $(U_{\text{exit}}, V_{\text{exit}})$
    $final\_exits[OD] \leftarrow final\_exits[OD] \cup \{exit\_counts, CE, NE, SE\}$
end for
return $final\_exits$

argue the trips used by the participants deviate significantly from the shortest paths, which may provide reasoning as to why a large proportion of CEs do not coincide with SEs. Although consisting of only a tiny proportion, CEs with SE orders as large as 7/8 still suggest that some trips are largely inefficient in terms of travel time. This phenomenon did not seem to improve from 2007/08 (when the I-35W dataset was collected) to 2010/11 (when the TBI dataset was collected). The total percentage of final exits on the shortest path dropped from 85.50% to 79.88%. Despite more people being exposed to advanced navigation systems over the 2–3 years (especially after the release of the Google Maps phone app on September 2008), the usage of the shortest path has not seen improvements. This lagging effect on technological advancement possibly indicates that people are reluctant to change their regular routines.

The NEs, on the other hand, are observed to have relatively low ratios, which may result from people intentionally skipping the CE due to other external factors. For instance, the driver may perceive that the CE is congested or wish to fuel their car by taking a different route. Regardless of the cause, the drivers are assumed to fully understand the consequences of skipping the CE and thus are not accounted for missing it. After deducting these trips, only 0.40% in the I-35W dataset and 1.22% in the TBI dataset are regarded as NEs. By applying the 25% threshold, 12 trips remain to be determined to contain missed exits, the 15% threshold yields 3 trips, while 5% yields 2 trips. As expected, the occurrence of missing exits only consists of a small portion of the total trips. It is worth noting that this analysis is independent of the rest of the paper, which focuses on the cost of missing a freeway exit. The extracted missed exits are not used as samples for any other analysis.

References

Ahmed, K.I., 1999. Modeling Drivers' Acceleration and Lane Changing Behavior (Ph.D. thesis). Massachusetts Institute of Technology.

Ahn, S., Cassidy, M.J., 2007. Freeway Traffic oscillations and Vehicle lane-Change Maneuvers.

Axhausen, K.W., Schönfelder, S., Wolf, J., Oliveira, M., Samaga, U., 2003. 80 Weeks of GPS-traces: Approaches to enriching the trip information. p. 29.

Azevedo, J., Santos Costa, M.E.O., Silvestre Madeira, J.J.E.R., Vieira Martins, E.Q., 1993. An algorithm for the ranking of shortest paths. European J. Oper. Res. 69 (1), 97–106.

Baccelli, F., Klein, M., Lebourges, M., Zuyev, S., 1997. Stochastic geometry and architecture of communication networks. Telecommun. Syst. 7 (1), 209–227.

Barceló, J. (Ed.), 2010. Fundamentals of traffic simulation. In: International Series in Operations Research & Management Science, vol. 145, Springer, New York, NY.

Carrion, C., Levinson, D., 2012. Value of travel time reliability: A review of current evidence. Transp. Res. A: Policy Pract. 46 (4), 720–741.

Chen, C., Gong, H., Lawson, C., Bialostozky, E., 2010. Evaluating the feasibility of a passive travel survey collection in a complex urban environment: Lessons learned from the New York City case study. Transp. Res. A: Policy Pract. 44 (10), 830–840.

Daley, D.J., Vere-Jones, D., 2008. An introduction to the theory of point processes. In: Gani, J., Heyde, C.C., Jagers, P., Kurtz, T.G. (Eds.), In: Probability and Its Applications, Springer, New York, NY.

Dia, H., 2002. An agent-based approach to modelling driver route choice behaviour under the influence of real-time information. Transp. Res. C 10 (5), 331–349.

Fox, J., 2008. Applied Regression Analysis and Generalized Linear Models, second ed Sage Publications, Inc, Thousand Oaks, CA, US.

Gao, Y., Levinson, D., 2023. Lane changing and congestion are mutually reinforcing? Commun. Transp. Res. 3, 100101.

Gipps, P.G., 1986. A model for the structure of lane-changing decisions. Transp. Res. B 20 (5), 403–414.

Gong, H., Chen, C., Bialostozky, E., Lawson, C.T., 2012. A GPS/GIS method for travel mode detection in New York City. Comput. Environ. Urban Syst. 36 (2), 131–139.

Halati, A., Lieu, H., Walker, S., 1997. Corsim - Corridor Traffic Simulation Model.

Hou, Y., Edara, P., Sun, C., 2012. A genetic fuzzy system for modeling mandatory lane changing. In: 2012 15th International IEEE Conference on Intelligent Transportation Systems. pp. 1044–1048. http://dx.doi.org/10.1109/ITSC.2012.6338877.

Hou, Y., Edara, P., Sun, C., 2014. Modeling mandatory lane changing using Bayes classifier and decision trees. IEEE Trans. Intell. Transp. Syst. 15 (2), 647–655.

Hunt, J.G., Lyons, G.D., 1994. Modelling dual carriageway lane changing using neural networks. Transp. Res. C 2 (4), 231–245.

Ji, A., Levinson, D., 2020. A review of game theory models of lane changing. Transportmetrica A: Transp. Sci. 16 (3), 1628–1647.

Ji, A., Levinson, D., 2021. Estimating the social gap with a game theory model of lane changing. IEEE Trans. Intell. Transp. Syst. 22 (10), 6320–6329.

Ji, A., Ramezani, M., Levinson, D., 2023a. Joint modelling of longitudinal and lateral dynamics in lane-changing maneuvers. Transportmetrica B: Transp. Dyn. 11 (1), 996–1025.

Ji, A., Ramezani, M., Levinson, D., 2023b. Pricing lane changes. Transp. Res. C 149, 104062.

Jiang, G., Fosgerau, M., Lo, H.K., 2020. Route choice, travel time variability, and rational inattention. Transp. Res. B 132, 188–207.

Kita, H., 1999. A merging–giveway interaction model of cars in a merging section: a game theoretic analysis. Transp. Res. A: Policy Pract. 33 (3), 305–312.

Leshed, G., Velden, T., Rieger, O., Kot, B., Sengers, P., 2008. In-car gps navigation: engagement with and disengagement from the environment. In: Proceedings of the SIGCHI Conference on Human Factors in Computing Systems. CHI '08, Association for Computing Machinery, New York, NY, USA, pp. 1675–1684.

Li, Z., Hensher, D.A., Rose, J.M., 2010. Willingness to pay for travel time reliability in passenger transport: A review and some new empirical evidence. Transp. Res. E: Logist. Transp. Rev. 46 (3), 384–403.

Liu, X., 2012. Survival Analysis: Models and Applications. John Wiley & Sons.

Schakel, W.J., Knoop, V.L., van Arem, B., 2012. Integrated lane change model with relaxation and synchronization. Transp. Res. Rec. 2316 (1), 47–57.

Stoyan, D., Kendall, W.S., Chiu, S.N., Mecke, J., 2013. Stochastic Geometry and Its Applications. John Wiley & Sons.

Tang, W., Levinson, D.M., 2018. Deviation between actual and shortest travel time paths for commuters. J. Transp. Eng. A: Syst. 144 (8), 04018042.

Toledo, T., Choudhury, C.F., Ben-Akiva, M.E., 2005. Lane-changing model with explicit target lane choice. Transp. Res. Rec. 1934 (1), 157–165.

Toledo, T., Koutsopoulos, H.N., Ben-Akiva, M.E., 2003. Modeling integrated lane-changing behavior. Transp. Res. Rec. 1857 (1), 30–38.

Toledo, T., Koutsopoulos, H.N., Ben-Akiva, M., 2007. Integrated driving behavior modeling. Transp. Res. C 15 (2), 96–112.

US Census Bureau, 2022a. Longitudinal employer-household dynamics.

US Census Bureau, 2022b. TIGER/Line Shapefiles.

Wang, H., Moylan, E., Levinson, D.M., 2022. Prediction of the deviation between alternative routes and actual trajectories for bicyclists. Findings.

Xie, F., Levinson, D., 2007. Measuring the structure of road networks. Geograph. Anal. 39 (3), 336–356.

Yang, C., Gidófalvi, G., 2018. Fast map matching, an algorithm integrating hidden Markov model with precomputation. Int. J. Geogr. Inf. Sci. 32 (3), 547–570.

Yang, Q., Koutsopoulos, H.N., 1996. A Microscopic Traffic Simulator for evaluation of dynamic traffic management systems. Transp. Res. C 4 (3), 113–129.

Zhang, Q., Langari, R., Tseng, H.E., Filev, D., Szwabowski, S., Coskun, S., 2020. A game theoretic model predictive controller with aggressiveness estimation for mandatory lane change. IEEE Trans. Intell. Veh. 5 (1), 75–89.

Zheng, Z., 2014. Recent developments and research needs in modeling lane changing. Transp. Res. B 60, 16–32.

Zheng, Z., Ahn, S., Chen, D., Laval, J., 2013. The effects of lane-changing on the immediate follower: Anticipation, relaxation, and change in driver characteristics. Transp. Res. C 26, 367–379.

Zhu, S., Levinson, D., 2015. Do people use the shortest path? An empirical test of Wardrop's first principle. PLOS ONE 10 (8), e0134322.

Zhu, S., Levinson, D., Liu, H.X., Harder, K., 2010. The traffic and behavioral effects of the I-35W Mississippi River bridge collapse. Transp. Res. A: Policy Pract. 44 (10), 771–784.